Cell

Article

Endogenous Hydrogen Sulfide Production Is Essential for Dietary Restriction Benefits

Christopher Hine,[1] Eylul Harputlugil,[1] Yue Zhang,[1] Christoph Ruckenstuhl,[4] Byung Cheon Lee,[2] Lear Brace,[1] Alban Longchamp,[1,3] Jose H. Treviño-Villarreal,[1] Pedro Mejia,[1] C. Keith Ozaki,[3] Rui Wang,[6] Vadim N. Gladyshev,[2] Frank Madeo,[4,5] William B. Mair,[1] and James R. Mitchell[1,*]

[1]Department of Genetics and Complex Diseases, Harvard School of Public Health
[2]Division of Genetics, Department of Medicine
[3]Department of Surgery and the Heart and Vascular Center
Brigham and Women's Hospital and Harvard Medical School, Boston, MA 02115, USA
[4]Institute for Molecular Biosciences, NAWI Graz, University of Graz, Graz 8010, Austria
[5]BioTechMed Graz, Humboldtstrasse 50, Graz 8010, Austria
[6]Department of Biology, Lakehead University, Thunder Bay, ON P7B 5E1, Canada
*Correspondence: jmitchel@hsph.harvard.edu
http://dx.doi.org/10.1016/j.cell.2014.11.048

SUMMARY

Dietary restriction (DR) without malnutrition encompasses numerous regimens with overlapping benefits including longevity and stress resistance, but unifying nutritional and molecular mechanisms remain elusive. In a mouse model of DR-mediated stress resistance, we found that sulfur amino acid (SAA) restriction increased expression of the transsulfuration pathway (TSP) enzyme cystathionine γ-lyase (CGL), resulting in increased hydrogen sulfide (H_2S) production and protection from hepatic ischemia reperfusion injury. SAA supplementation, mTORC1 activation, or chemical/genetic CGL inhibition reduced H_2S production and blocked DR-mediated stress resistance. In vitro, the mitochondrial protein SQR was required for H_2S-mediated protection during nutrient/oxygen deprivation. Finally, TSP-dependent H_2S production was observed in yeast, worm, fruit fly, and rodent models of DR-mediated longevity. Together, these data are consistent with evolutionary conservation of TSP-mediated H_2S as a mediator of DR benefits with broad implications for clinical translation.

INTRODUCTION

Dietary restriction (DR) encompasses a variety of nutritional interventions with overlapping functional benefits including increased stress resistance and extended longevity in a number of organisms across evolutionary boundaries (Fontana et al., 2010). In mammals, dietary regimens associated with these benefits are diverse, including reduced daily food intake, intermittent fasting and reduced protein or essential amino acid intake. Although common features exist among DR regimens, including reduced adiposity and improved sensitivity to growth factors, differences exist as well. Thus, whether overlapping functional benefits of DR regimens share a common underlying nutritional and/or molecular basis remains unclear. Despite strong evidence of DR benefits in humans (Levine et al., 2014), difficulties with compliance prevent widespread clinical applications. Uncovering common mechanisms is thus of great significance for targeted dietary and/or pharmacological interventions.

Mitohormesis represents a potential unifying molecular hypothesis of DR action (Sinclair, 2005). Based on the concept of hormesis (Calabrese and Mattson, 2011), in which low-level stressors promote adaptive changes resulting in stress resistance, the mitohormesis hypothesis of DR posits that increased reactive oxygen and nitrogen species (RONS) derived from increased mitochondrial fatty acid oxidation induce mild oxidative stress, thus driving adaptive mechanisms of antioxidant protection (Tapia, 2006). SKN1/NRF2 has emerged as a candidate mediator of adaptive protection based on its activation by RONS and function as a key transcription factor in the cytoprotective phase II antioxidant and detoxification response (Hine and Mitchell, 2012). Gene targets of NRF2 include heme oxygenase-1 (HO-1), NAD(P)H dehydrogenase quinone 1 (NQO-1), glutathione transferases (GSTs), and additional genes that utilize glutathione (GSH) for resolving oxidative stress. SKN1/NRF2 in worms is required for stress resistance and longevity benefits of DR (Bishop and Guarente, 2007). In mammals, NRF2 is required for DR-mediated protection from chemically induced carcinogenesis but not for DR-mediated longevity (Pearson et al., 2008). Functionally, mitohormesis can be blocked by vitamin C, vitamin E, and/or N-acetyl cysteine (NAC), presumably due to their antioxidant capacity (Ristow and Schmeisser, 2011).

Restriction of sulfur amino acids (SAAs) methionine (Met) and cysteine (Cys) is common to numerous DR regimens across evolutionary boundaries and is thus a potential shared nutritional trigger of DR benefits. In yeast, Met restriction extends longevity (Ruckenstuhl et al., 2014). In flies, restriction of essential amino acids (EAAs), and in particular Met, controls DR longevity benefits (Grandison et al., 2009). Dietary Met further interacts with overall protein levels in longevity control (Lee et al., 2014). In rodents, diets lacking the nonessential amino acid (NEAA) Cys and restricted for Met (Met restriction, or MetR) extend longevity and increase hepatic stress resistance (Miller et al., 2005; Orentreich et al., 1993).

The TSP controls the conversion of Met into Cys and is required for DR-mediated lifespan extension in flies (Kabil et al., 2011a). Two key enzymes of this evolutionarily conserved pathway are cystathionine β-synthase (CBS) and cystathionine γ-lyase (CGL). Under normal physiological conditions, CBS converts serine and homocysteine, a product of Met methyl transfer, into cystathionine. Cystathionine is then converted into α-ketobutyrate and Cys by CGL (Kabil et al., 2011b). Although Cys is required for de novo synthesis of GSH, thus potentially linking TSP to NRF2-mediated antioxidant responses, the molecular mechanism underlying the genetic requirement for a functional TSP in DR-mediated benefits is unknown.

A product of the TSP with potential to mediate physiological benefits including stress resistance and extended longevity is the water and fat-soluble gas H_2S (Cuevasanta et al., 2012; Zhang et al., 2013). Although toxic at high levels, H_2S produced at low concentrations by degradation of Cys or homocysteine by CGL or CBS acts on the vasculature and the brain as a signaling molecule to reduce blood pressure (Yang et al., 2008) and prevent neurodegeneration (Paul and Snyder, 2012). Exogenous H_2S can also extend lifespan of worms (Miller and Roth, 2007) and induce suspended animation in mammals (Blackstone et al., 2005). Although diet can impact H_2S production (Predmore et al., 2010), neither the dietary requirements for increased endogenous H_2S production, nor the potential role of H_2S in the benefits of DR are currently known.

Ischemia reperfusion injury (IRI) is initiated by lack of nutrients and oxygen due to occlusion of blood flow (ischemia) followed by activation of pro-oxidation pathways and inflammatory mediators in damaged tissues upon return of blood flow (reperfusion). IRI represents a major clinical concern in controlled (tissue resection, organ transplantation) and uncontrolled settings (stroke, heart attack). Various short-term (3–14 days) DR regimens improve outcome in models of kidney, liver, and brain IRI (Harputlugil et al., 2014; Mitchell et al., 2010; Peng et al., 2012; Varendi et al., 2014). Here, we used dietary preconditioning against hepatic IRI as a model system to probe dietary and molecular mechanisms underlying protection.

RESULTS

NAC, but Not NRF2 Deficiency, Abrogates Benefits of DR against IRI

Fifty percent DR for 7 days significantly decreased body weight, percentage fat mass, serum triglycerides (TGs) (Figures 1A–1C), and blood glucose (BG) (Figure S1A available online) while increasing hepatic expression of FAO-related genes (Figure 1D) and the rate of peroxisomal FAO (Figure 1E) relative to the ad libitum (AL)-fed group. Consistent with the mitohormesis hypothesis, hepatic RONS and NRF2 target gene expression were increased (Figures 1F and 1G), and the latter blocked by NAC administration during the DR period. Total GSH was also decreased upon DR (Figure 1H).

The functional relevance of increased RONS and NRF2 activation in DR-mediated stress resistance was tested in a model of hepatic IRI. Wild-type (WT) mice were preconditioned on AL or DR regimens ± NAC for 1 week prior to IRI. NAC treatment was halted 24 hr prior to IRI to avoid any direct antioxidant effects of this short-lived compound on outcome. Neither DR nor NAC had any significant effect on liver damage markers in serum prior to IRI (data not shown). After reperfusion, liver damage markers remained significantly lower in DR serum indicative of protection from injury (Figure 1I). NAC had no effect on outcome in the AL group, but significantly reduced protection in the DR group. Macroscopic and histological analysis of hemorrhagic necrosis in livers excised 24 hr after reperfusion (Figure 1J; Figure S1B) was consistent with serum damage markers (Figure 1I).

To test the requirement for the NRF2-dependent phase II antioxidant response, we compared NRF2 knockout (KO) mice to wild-type (WT) littermate controls. NRF2KO mice subjected to DR had decreased hepatic GSH similar to WT (Figure S1C) but failed to upregulate phase II antioxidant response genes as expected (Figure S1D). Surprisingly, benefits of DR against hepatic IRI did not require NRF2, with similar reductions in liver damage markers in serum (Figure 1K) and macroscopic evidence of hemorrhage 24 hr postreperfusion upon DR in both WT and NRF2KO mice (Figure S1E). To confirm and extend this result, we tested the requirement for NRF2 in DR-mediated protection from renal IRI. Although AL-fed NRF2KOs had slightly elevated damage and decreased renal function upon IRI relative to WT mice as reported previously (Liu et al., 2009), both gained similar benefits upon DR (Figure S1F).

Sulfur Amino Acids Control the Benefits of DR and PR

NRF2 independence of DR benefits despite abrogation by NAC is consistent either with an alternate RONS-dependent mechanism of DR-mediated protection, or an antioxidant-independent activity of NAC. NAC is also a source of Cys, and NAC supplementation to the DR group above serendipitously returned dietary Cys content close to AL levels. To separate the functional consequences of antioxidant capacity from SAA content, we supplemented restricted diets separately with either antioxidants (vitamin C and E [VitC&E]) or a 2 × concentration of Met and Cys (2×Met&Cys) for 1 week prior to hepatic IRI. Following reperfusion, protection afforded by DR was maintained despite VitC&E antioxidant treatment, but abrogated by 2×Met&Cys (Figures 2A and 2B) without affecting food intake, weight loss, or expression of FOXO target genes (Figures S2A–S2C), consistent with the relative importance of the SAA aspect of NAC in abrogation of DR benefits.

Protein and carbohydrates are isocaloric and partially interconvertible as dietary energy sources, rendering distinctions between calorie restriction and protein/amino acid restriction upon DR challenging. To test the relative contribution of energy restriction, protein restriction (PR), and specifically SAA restriction to DR-mediated protection against hepatic IRI, we preconditioned mice on a complete or isocaloric protein-free diet fed either AL or 35% restricted ± 2×Met&Cys. Following hepatic IRI, PR mice displayed significant protection from liver damage (Figures 2C and 2D) independent of total calorie intake or weight loss (Figures S2D and S2E). Importantly, 2×Met&Cys abrogated significant benefits of combined protein/energy restriction (Figures 2C and 2D) without affecting weight loss (Figure S2E). Because MetR regimens offering overlapping functional benefits with DR are also restricted or deficient in Cys, we also tested Cys reconstitution alone. Following reperfusion, protection observed

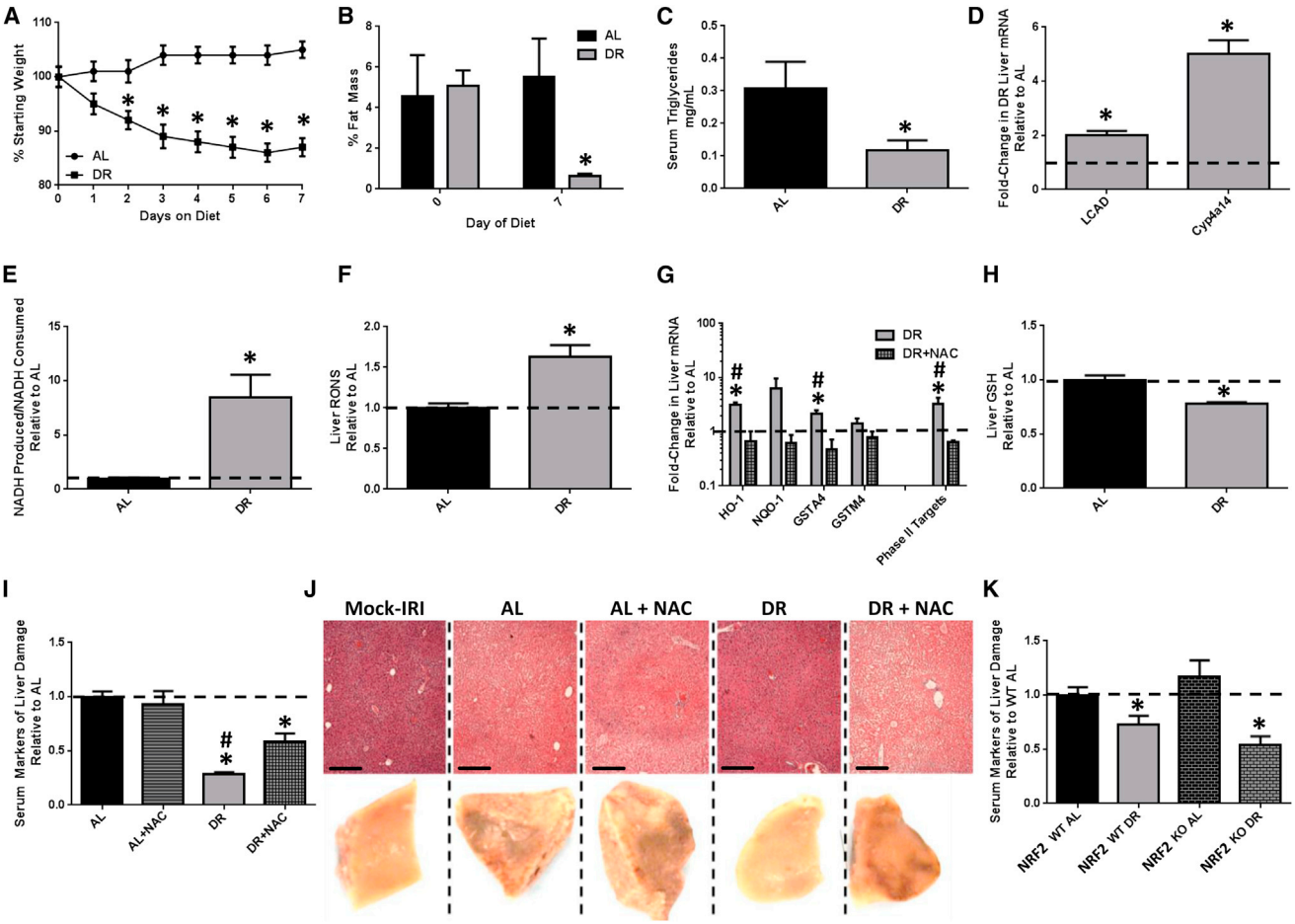

Figure 1. NAC Abrogates Benefits of DR against Acute Stress Independent of NRF2

(A–H) Effects of 1 week of 50% DR versus AL feeding ± NAC as indicated on body weight (n = 15–17/group, A); %fat mass (n = 5/group, B); serum triglycerides (n = 4–7/group, C); hepatic FAO-associated gene expression (n = 3/group, D); peroxisomal FAO capacity in liver extracts (n = 3/group, E); hepatic RONS (n = 6–8/group, F); hepatic NRF2 target gene expression (n = 4/group, G); and hepatic GSH levels (n = 7/group, H).

(I and J) Combined serum markers of liver damage normalized to the average of the AL control group (I) and liver pathology from injured left liver lobes on the microscopic level stained with hematoxylin and eosin (scale bar, 250 μm, above) and the macroscopic level (1× magnification, below) showing fixed tissue 24 hr after reperfusion (J) in mice (n = 5–6/group) preconditioned as indicated before hepatic IRI or mock injury. Asterisk indicates the significance of the difference between AL and DR, and pound sign between DR and DR + NAC; */#$p < 0.05$.

(K) Serum markers of liver damage in WT (n = 5–6/group) or NRF2KO (n = 7–12/group) preconditioned as indicated. Asterisk indicates the significance of the difference between AL and DR within genotype; *$p < 0.05$.

All error bars SEM. See also Figure S1.

in the DR group was abrogated upon 2×Cys supplementation (Figures 2E and 2F), consistent with PR and Cys restriction as critical aspects of DR-mediated resistance to hepatic IRI.

DR Stimulates Endogenous H_2S Production via Repression of mTORC1 and Activation of the TSP

Expression and activity of TSP genes CBS and CGL increase when Cys is low (Stipanuk and Ueki, 2011) to allow de novo synthesis from Met (Figure 3A). Hepatic CGL and CBS to a lesser degree were increased on the mRNA and protein levels upon 1 week DR (Figures 3B and 3C), and this was abrogated by 2× Met&Cys or NAC supplementation (Figure 3B).

A metabolomics approach was used to identify candidate TSP metabolites involved in DR-mediated protection. To facilitate identification of potentially causative versus correlative changes, we included a genetic model that fails to gain the benefits of DR against hepatic IRI due to liver-specific genetic ablation of the mTORC1 repressor, tuberous sclerosis complex 1 (TSC1) (Harputlugil et al., 2014) (Figure 3D; Figure S3A). GSH and taurine are two downstream metabolites with potential to protect against IRI, however neither was increased by DR specifically in WT mice (Figure 3D). A third protective TSP metabolite is hydrogen sulfide (H_2S) (Kang et al., 2009). Although not detected in our metabolomic screen, associated by-products homoserine and serine (Kabil et al., 2011b) were significantly increased upon DR in WT but not TSC1KO livers (Figure 3D).

For direct measurement of H_2S, we leveraged the specific reaction between H_2S and lead acetate to form a black precipitate

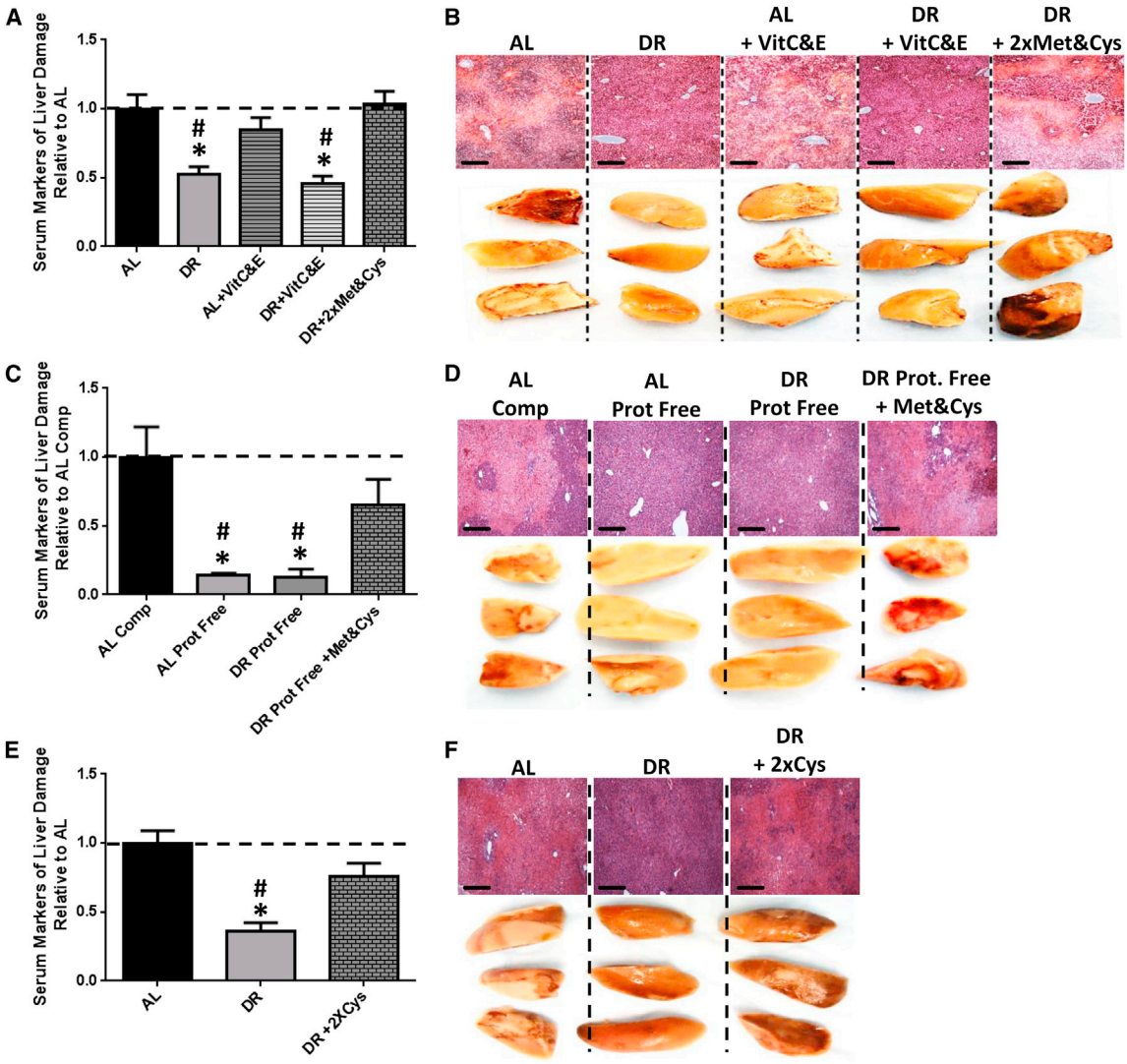

Figure 2. Sulfur Amino Acids Control the Benefits of DR and PR

(A and B) Serum markers of liver damage (A) and liver pathology after reperfusion (B) in mice (n = 5/group) preconditioned on complete diets fed AL or 50% DR ± supplementation with vitamins C&E or Met&Cys as indicated. Asterisk indicates the significance of the difference versus AL and pound sign versus DR + 2× Met&Cys; */#$p < 0.05$.

(C and D) Serum markers of liver damage (C) and liver pathology after reperfusion (D) in mice (n = 5/group) preconditioned on complete (Comp) or protein-free (Prot. Free) diets fed AL or 35% DR with Met&Cys addition as indicated prior to hepatic IRI. Asterisk indicates the significance of the difference versus AL complete and pound sign versus DR Prot. Free + Met&Cys; */# $p < 0.05$.

(E and F) Serum markers of liver damage (E) and liver pathology after reperfusion (F) in mice (n = 5/group) preconditioned on complete diets fed AL or 50% DR with 2×Cys added as indicated. Asterisk indicates the significance of the difference versus AL and pound sign versus DR + 2×Cys; */#$p < 0.05$.

All error bars SEM. See also Figure S2.

(lead sulfide) that can be trapped and visualized on filter paper containing lead acetate (Figure S3B). In the presence of excess CGL/CBS substrate Cys and cofactor pyridoxal-5′-phosphate (PLP), H_2S gas produced by liver extracts was greater from DR- than AL-fed mice (Figure 3E). This phenomenon was independent of NRF2 status (Figure S3C). Met&Cys add-back during DR blocked the DR-mediated increase in H_2S production capacity (Figure 3F), correlating with a loss of protection against hepatic IRI (Figure 2A) and normalization of hepatic GSH levels (Figure S3D).

Using a less specific but more easily quantifiable sulfide probe-based method calibrated against known H_2S concentrations (Figures S3E and S3F), liver extracts of DR mice displayed a 4-fold increase in H_2S production capacity compared to AL mice (Figure 3G). Endogenous hepatic H_2S levels measured by insertion of the sulfide probe into the right and median lobes of anesthetized mice were in the low micromolar range relative to the appropriate standard curve (Figures S3G and S3H), and nearly 3-fold higher in the livers of DR relative to AL-fed mice (Figure 3H).

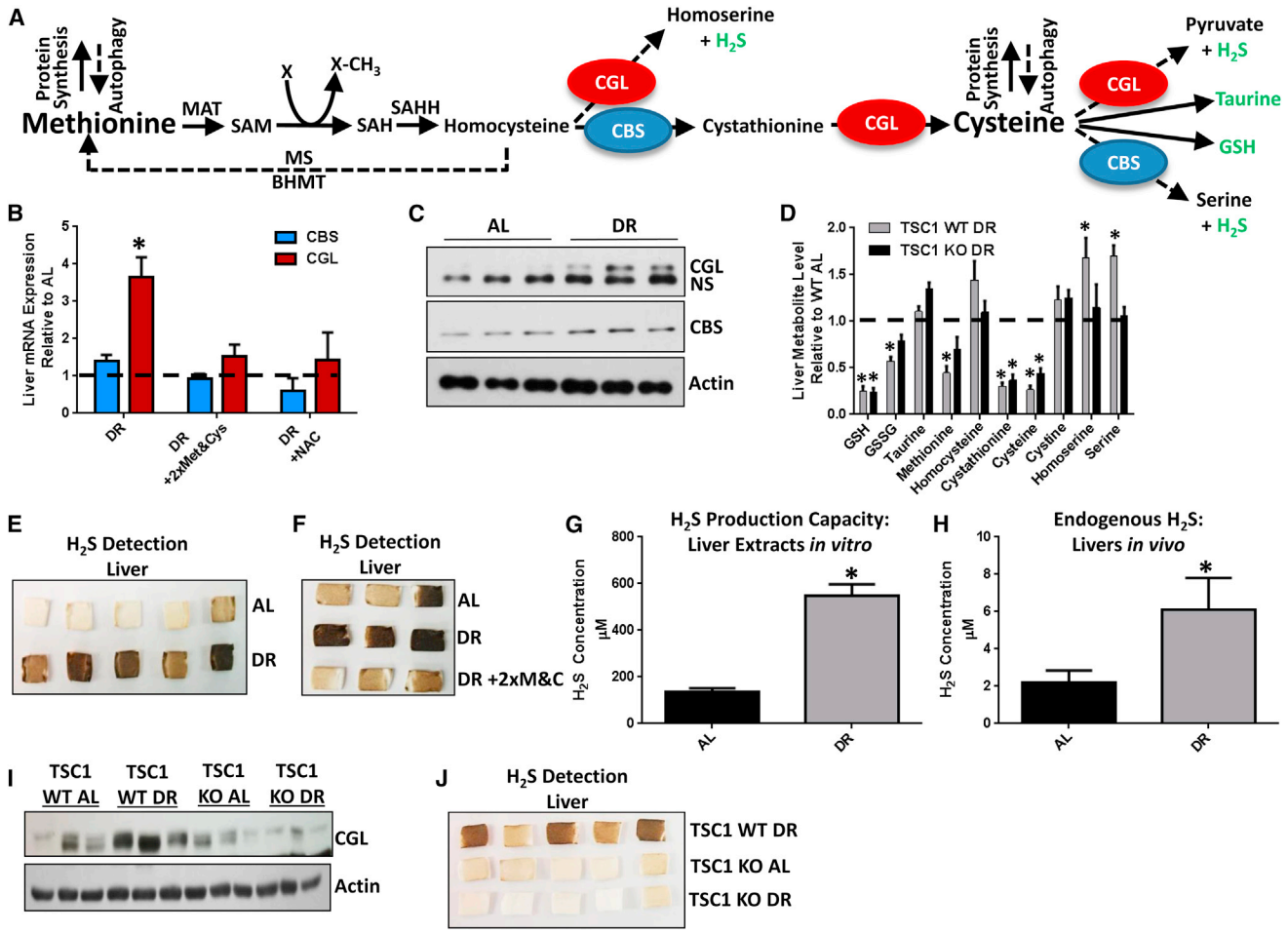

Figure 3. DR Stimulates Endogenous H_2S Production via the TSP

(A) Model of the transmethylation and TSP. Arrows trace sulfur from Met to Cys and downstream cellular processes via cystathionine beta-synthase (CBS) and cystathionine gamma-lyase (CGL). Metabolites in green (taurine, GSH and H_2S) have demonstrated potential to protect against IRI. MAT, methionine adenosyl transferase; SAM: S-adenosylmethionine; SAH, S-adenosylhomocysteine; SAHH, S-adenosylhomocysteine hydrolase; MS, methionine synthase; BHMT, betaine homocysteine methyltransferase.

(B) Hepatic CBS and CGL gene expression upon DR ± 2×Met&Cys or NAC as indicated; n = 3/group.

(C) Immunoblots of CGL, CBS, and actin in liver extracts from AL or DR mice as indicated; NS, nonspecific protein band.

(D) Liver metabolites in WT or LTsc1KO mice fed 35% DR on a protein-free diet relative to the AL-fed complete diet group; n = 5/group.

(E and F) H_2S production capacity from liver extracts of AL or DR mice (E) ± 2×Met&Cys (F) as detected by the black precipitate, lead sulfide.

(G) H_2S production capacity as in (E) but using a microsulfide probe to detect H_2S.

(H) Endogenous hepatic H_2S in mice on the indicated diet using a microsulfide probe inserted into liver lobes; n = 3 mice/group, two lobes/mouse. Asterisk indicates the significance of the difference versus AL; *$p < 0.05$.

(I and J) Immunoblots of liver CGL (I) and H_2S production (J) in WT and LTsc1KO mice fed AL or 35% DR on a protein-free diet.

All error bars SEM. See also Figure S3.

Consistent with a link between DR, TSP, H_2S, and protection from IRI, DR failed to increase hepatic CGL protein and H_2S production capacity in livers of TSC1KO mice (Figures 3I and 3J), suggesting that constitutive mTORC1 activation blocks DR-mediated TSP upregulation.

H_2S Is Necessary and Sufficient to Confer DR-Mediated Stress Resistance In Vivo

We next determined if exogenous H_2S is sufficient to confer protection in our model of hepatic IRI. AL-fed mice injected with the H_2S precursor NaHS or vehicle 30 min prior to ischemia had decreased liver damage relative to vehicle-treated controls (Figures 4A and 4B). Similarly, noninvasive H_2S delivery in the drinking water for 1 week prior to hepatic IRI using the slow releasing/long-lived donor GYY4137 (Lee et al., 2011) (but not the fast releasing/short-lived donor NaHS) decreased liver damage without affecting animal weight, food intake, or water consumption (Figures S4A–S4D). Thus, exogenous H_2S is sufficient to protect against hepatic IRI.

A specific inhibitor of CGL, DL-propargylglycine (PAG), was employed to determine if endogenous H_2S is necessary for DR-mediated stress resistance. PAG treatment blocked hepatic

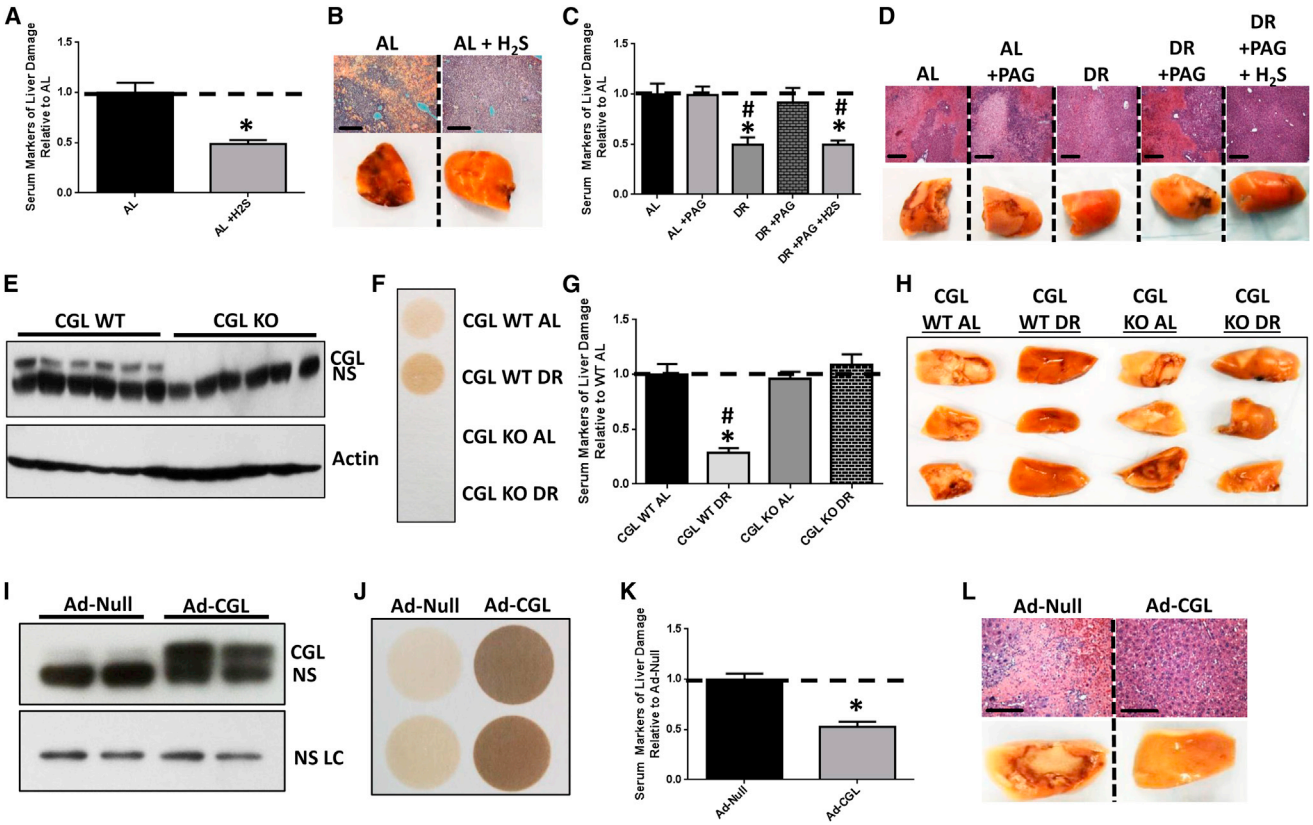

Figure 4. H_2S Is Necessary and Sufficient to Confer DR Benefits against Hepatic IRI

(A and B) Serum markers of liver damage (A) and liver pathology after reperfusion (B) in mice (n = 4–5/group) treated with vehicle or H_2S 30 min prior to surgery. Asterisk indicates the significance of the difference versus AL; *p < 0.05.

(C and D) Serum markers of liver damage (C) and liver pathology after reperfusion (D) in mice (n = 3–4/group) treated with PAG during AL or DR preconditioning with a single H_2S injection prior to surgery as indicated. Asterisk indicates the significance of the difference versus AL and pound sign versus DR + PAG; */#p < 0.05.

(E) Immunoblot of CGL in liver extracts of WT or CGLKO mice as indicated. NS, nonspecific protein.

(F) H_2S production capacity of liver extracts from WT or CGLKO mice preconditioned as indicated.

(G and H) Serum markers of liver injury (G) and liver pathology after reperfusion (H) in WT or CGLKO mice (n = 5–8/group) preconditioned as indicated. Asterisk indicates the significance of the difference versus WT AL and pound sign versus CGLKO DR; */#p < 0.05.

(I) Immunoblot of CGL in liver extracts from WT mice infected with control (Ad Null) or CGL-overexpressing (Ad-CGL) adenovirus as indicated; NS LC, nonspecific loading control protein.

(J) H_2S production capacity of liver extracts of Ad-Null- or Ad-CGL-infected mice.

(K and L) Serum markers of liver damage (K) and liver pathology after reperfusion (L) in Ad-Null- or Ad-CGL-infected mice (n = 6/group). Asterisk indicates the significance of the difference versus Ad Null; *p < 0.05.

All error bars SEM. See also Figure S4.

H_2S production capacity (Figure S4E) and decreased endogenous hepatic H_2S levels upon DR (Figure S4F), consistent with the dominant role of CGL in hepatic H_2S production. PAG treatment had no effect on IRI outcome in AL mice but abrogated benefits of DR (Figures 4C and 4D). Readdition of H_2S via IP injection of 30 min prior to induction of ischemia in DR + PAG-treated mice restored protection (Figures 4C and 4D).

Two genetic models were used to test the specificity of the TSP and H_2S in protection against hepatic IRI (Figures 4E–4L). The necessity of CGL in DR-mediated benefits was tested with whole-body CGLKO mice (Yang et al., 2008). CGLKO mice responded to DR like WT mice with respect to changes in body weight, food intake, body composition, and blood glucose (Figures S4G–S4J) despite the lack of CGL protein in liver or capacity of liver extracts to produce H_2S (Figures 4E and 4F). However, whereas the absence of CGL had no apparent impact on the outcome of hepatic IRI in AL-fed mice, CGLKO mice failed to gain protection upon DR (Figures 4G and 4H). To test the sufficiency of increased TSP activity and endogenous H_2S production, CGL was overexpressed via adenoviral-mediated gene delivery (Ad-CGL). Hepatic CGL protein levels and H_2S production capacity were both significantly increased (Figures 4I and 4J) independent of body mass or food intake relative to control adenovirus (Ad Null) -infected mice (Figures S4K and S4L). Ad-CGL infection resulted in improved outcome after hepatic IRI relative to Ad-Null-infected mice (Figures 4K and 4L). Together,

these results suggest that increased TSP activity and endogenous H_2S production via CGL are sufficient and, in the case of DR, necessary for protection against the acute surgical stress of hepatic IRI.

H_2S Is Necessary and Sufficient to Confer DR-Mediated Stress Resistance In Vitro via Sulfhydration and Antioxidant Properties

To determine if TSP gene expression and H_2S production can be induced in a cell-autonomous manner by SAA restriction, we cultured mouse hepatocyte-derived Hepa1-6 cells overnight in complete media or media lacking SAA (–Met&Cys). Similar to DR in vivo, SAA deprivation increased CBS and CGL expression and H_2S production capacity in vitro (Figures 5A and 5B).

To determine if exogenously added H_2S can protect cultured Hepa1-6 cells against simulated IRI, warm ischemia was simulated by replacing growth media with saline and incubating in a 37°C hypoxic chamber for up to 4 hr, and reperfusion by replacing the growth media under normoxic conditions. Addition of H_2S decreased Hepa1-6 cell damage under both normoxic and hypoxic conditions during the ischemic phase (Figure 5C) and restored MTT activity during the reperfusion phase (Figure 5D), indicating that exogenous H_2S is sufficient to induce significant protection against both nutrient/energy deprivation and hypoxia in vitro.

To assess if endogenous H_2S induced by SAA restriction afforded similar protection, primary hepatocytes were cultured ± Met&Cys overnight prior to simulated IRI. LDH release during ischemia was decreased (Figure 5E), and MTT activity during reperfusion increased in hepatocytes preconditioned in Met&Cys-deficient media (Figure 5F). Similar protection afforded by overnight preconditioning of Hepa1-6 cells in -Met&Cys media was blocked by addition of PAG during the preconditioning period and was partially rescued by exogenous addition of H_2S during ischemia (Figure S5A).

H_2S has been proposed to prevent cell damage/death under stress in part by sulfhydration of target proteins (Paul and Snyder, 2012) including the mitochondrial inner membrane component sulfide quinone oxidoreductase (SQR), which allows transfer of electrons from H_2S to coenzyme Q and the electron transport chain (ETC) (Módis et al., 2013; Olson et al., 2013) (Figure 5G). To test the potential role of the SQR in H_2S-mediated protection, we partially knocked down the SQR in Hepa1-6 cells (Figure S5B) prior to simulated IRI ± exogenous H_2S. H_2S addition reduced LDH release during the ischemic phase and upon reperfusion (Figures 5H and 5I); the latter was significantly altered upon SQR knockdown (KD) (Figure 5I). Additionally, the increase in MTT activity during the reperfusion phase in the presence of H_2S was significantly reduced by SQR KD (Figure 5J). SQR KD did not significantly alter the effects of H_2S addition on nutrient/growth factor withdrawal in the absence of hypoxia (Figures 5H–5J).

Because oxidation of H_2S by SQR results in production of thiosulfate ($S_2O_3^{-2}$) (Hildebrandt and Grieshaber, 2008), which itself can be utilized in mammalian tissues under hypoxic conditions for further H_2S production (Olson et al., 2013), we next tested if this downstream metabolite could afford similar protection against simulated IRI in Hepa1-6 cells. Although thiosulfate had a negative impact on LDH release upon nutrient/growth factor withdrawal under normoxia, increasing thiosulfate concentrations decreased cell damage during the ischemic phase under hypoxia (Figure S5C) and improved MTT activity during the reperfusion phase (Figure S5D). SQR KD partially blocked thiosulfate-mediated protection against simulated IRI (Figure 5K; Figure S5E), suggesting that the protective effect of thiosulfate during hypoxia can be partially attributed to its conversion to H_2S.

H_2S also has antioxidant properties (Calvert et al., 2010) that could contribute to cytoprotection independent of target protein sulfhydration. At 100 μM but not 10 μM final concentration, H_2S protected Hepa1-6 cells against acute oxidative stress delivered by H_2O_2 exposure (Figures S5F and S5G). Similar protection was found with 100 μM H_2S against H_2O_2 exposure in primary smooth muscle cells (Figures S5H and S5I). Thus, H_2S protects from acute ischemic insult and oxidative stress via multiple mechanisms.

Increased Endogenous H_2S Production in Diet-Induced Longevity Extension Models across Evolutionary Boundaries

Although exogenous H_2S can extend longevity in worms, the potential role of endogenous H_2S in DR-mediated lifespan extension has not been reported. To test the hypothesis that increased endogenous H_2S is a common feature of DR regimens that lead to extended longevity across evolutionary boundaries, we measured H_2S production capacity in four different organisms subjected to species-appropriate DR longevity regimens.

Adult mice subjected to long-term MetR (Figure 6A), EOD fasting, or 20%–30% DR (Figure 6B) had increased H_2S production capacity in liver and kidney extracts compared to AL-fed complete diet controls. In mice subjected to 1 week 50% DR, kidney, spleen, and carotid artery additionally demonstrated increased H_2S production capacity (Figure S6A), whereas brain, skeletal muscle, heart, and aorta tested under the same conditions did not (Figure S6B). Nonetheless, primary smooth muscle cells prepared from aorta displayed increased H_2S production capacity upon Met&Cys depletion (Figure S6C), suggesting tissue/cell type specificity in the regulation of the TSP in response to diet. Although we failed to observe an increase in H_2S production capacity in mouse brain upon 1 week 50% DR, 3 days of water-only fasting increased H_2S production capacity (Figure S6D).

In the fruit fly *D. melanogaster*, maximal H_2S production capacity of whole-body extracts of flies subjected to varying levels of dietary protein and Met restriction (Figure 6C) correlated with maximal lifespan extension (Lee et al., 2014).

In the nematode worm *C. elegans*, the *eat-2* mutant serves as a genetic model of lifespan extension by DR due to defects in pharyngeal function resulting in decreased food intake (Lakowski and Hekimi, 1998). Extracts of *eat-2* mutants produced more H_2S than extracts of age-matched WT N2 worms (Figure 6D). To assess the genetic requirements for TSP factors in longevity extension, we performed individual RNAi-mediated KD of the two worm CGL homologs CTH-1 and CTH-2, the CBS homolog CBS-1, and a fourth worm TSP gene, CBL-1. Individual RNAi KD of CBL-1 and CBS-1 had no effect on longevity

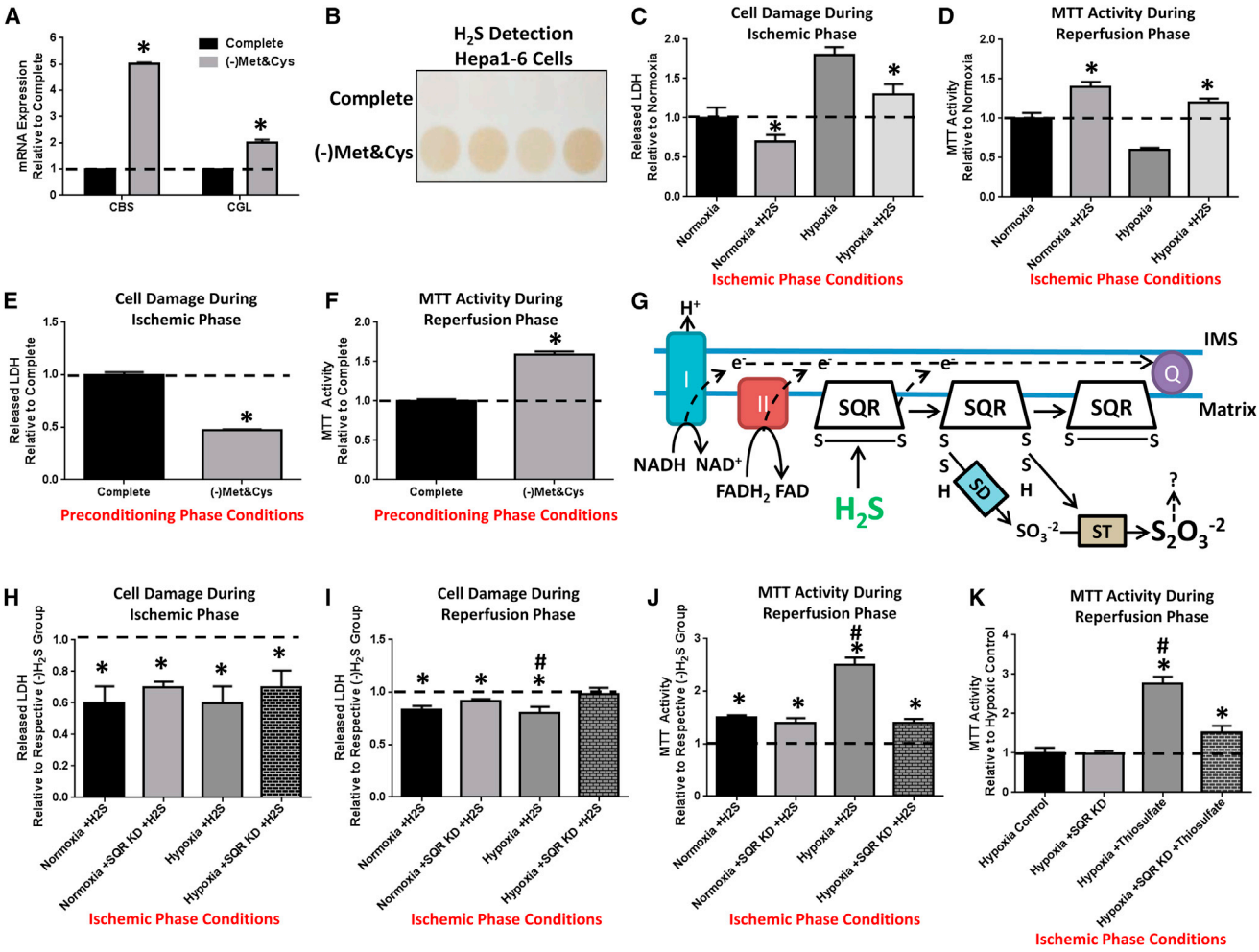

Figure 5. Mitochondrial SQR Is Required for Cytoprotective Effects of H_2S during Ischemia

(A and B) Cell-autonomous increase in TSP enzymes and H_2S production. (A) CBS and CGL gene expression in Hepa1-6 cells cultured overnight in complete or -Met&Cys media. Asterisk indicates the significance of the difference versus complete; *p < 0.05. (B) H_2S production in live Hepa1-6 cells preconditioned in complete or -Met&Cys media in quadruplicate for 16–24 hr as indicated before readdition of Cys and PLP for H_2S detection.

(C and D) Cell-autonomous effects of exogenous H_2S on simulated IRI in Hepa1-6 cells in vitro; H_2S was added during the ischemic phase and removed upon simulated reperfusion. (C) LDH release during the ischemic phase consisting of 3 hr incubation in saline (simulated nutrient/energy deprivation) under normoxic or hypoxic (simulated ischemia) conditions ± exogenous H_2S as indicated. (D) MTT activity during the reperfusion phase consisting of readdition of complete media under normoxic conditions (simulated reperfusion).

(E and F) Cell-autonomous effects of overnight Met&Cys withdrawal (preconditioning phase conditions) on simulated IRI in primary hepatocyes in vitro. LDH release (E) during simulated ischemia and MTT activity (F) upon simulated reperfusion.

(G) Schematic of H_2S oxidation to thiosulfate by SQR in mitochondria. Q, coenzyme Q; IMS, inner membrane space; I and II, complex I and II of the mitochondrial ETC; SD, sulfur dioxygenase; ST, sulfur transferase; $S_2O_3^{-2}$, thiosulfate.

(H–J) Effects of exogenous H_2S on simulated IRI upon SQR KD in Hepa1-6 cells. LDH release during the ischemic phase (H) in saline under the indicated normoxic or hypoxic conditions ± SQR KD, and during the reperfusion phase (I) in complete media expressed relative to respective group not receiving H_2S during the ischemic phase; and MTT activity (J) during the reperfusion phase. Asterisk indicates the significance of the difference in the indicated group ± H_2S treatment; hash mark indicates the significance of the difference between control and SQR KD within a given treatment group; */#p < 0.05.

(K) Cell-autonomous effects of exogenous thiosulfate on MTT activity during the reperfusion phase following simulated IRI in Hepa1-6 cells ± SQR KD. Asterisk indicates the significance of the difference in the indicated group ± thiosulfate treatment; hash mark indicates the significance of the difference between control and SQR KD within a given treatment group; */#p < 0.05.

All error bars SEM. See also Figure S5.

(Figure S6E), but RNAi KD specifically of CBS-1 significantly decreased *eat-2* mediated lifespan extension, whereas overexpression of CBS-1 significantly extended median lifespan of WT N2 controls (Figure 6F).

Finally, DR-mediated extension of chronological lifespan in the yeast *S. cerevisiae* can be accomplished by reducing glucose in the growth media from 2% to 0.5% (Figure 6G) (Wu et al., 2013). Under these conditions, H_2S production from the

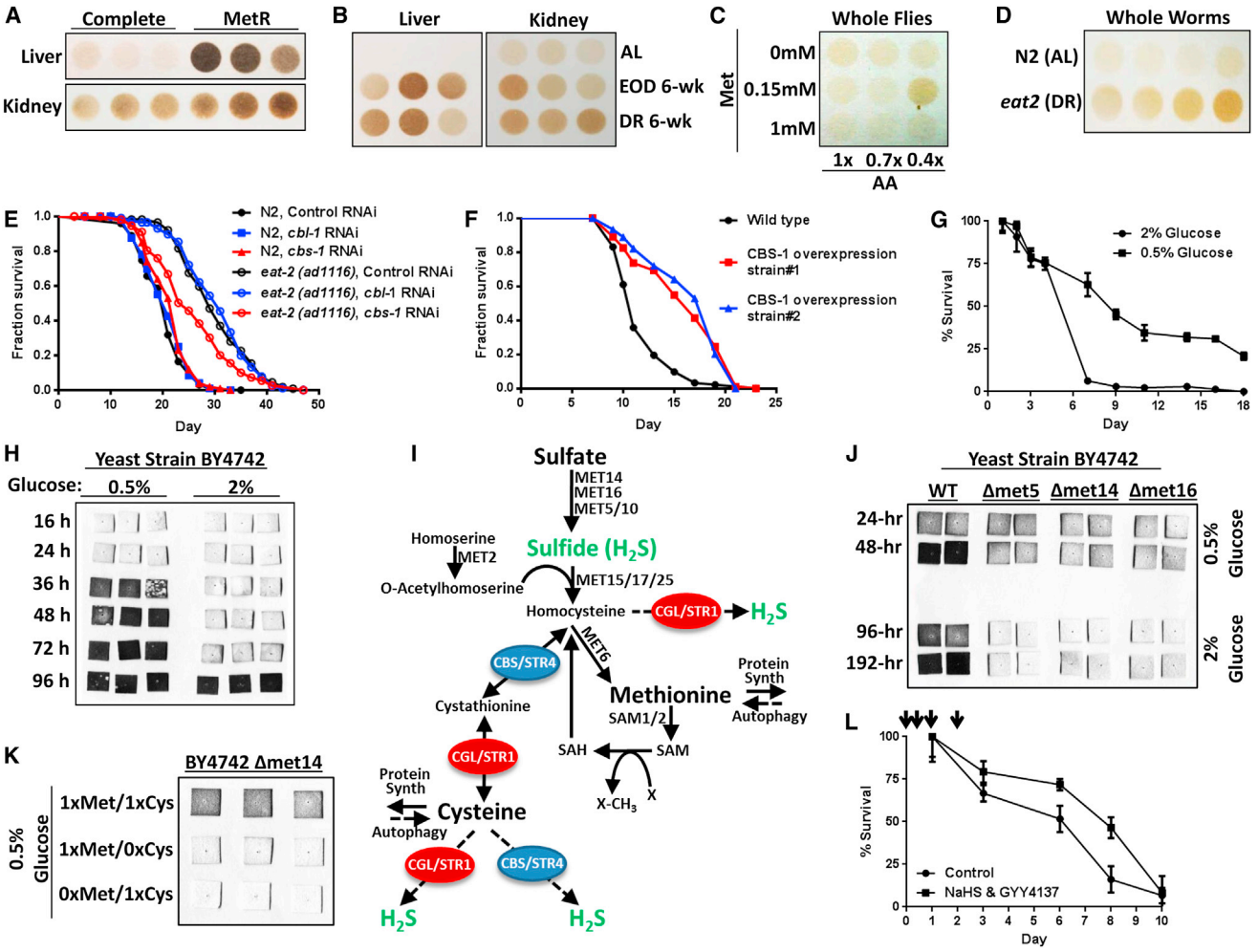

Figure 6. Increased Endogenous H_2S Production in Diet-Induced Longevity Extension Models Crosses Evolutionary Boundaries

(A and B) H_2S production capacity of liver and kidney extracts from mice with AL access to complete or MetR diets as indicated for 4 months (A) and in mice with AL, every-other-day (EOD) fasting, or 20%–30% restricted diets for 6 weeks (B). Each circle represents H_2S production from an individual animal, normalized for extract protein content.

(C) H_2S production capacity of whole-fly lysates normalized for protein content from populations subjected to the indicated dietary amino acid (AA) and Met concentrations. Maximal H_2S production capacity correlated with the optimal diet for longevity extension (0.4 × AA with 0.15 mM Met) (Lee et al., 2014).

(D) H_2S production capacity of N2 and *eat-2* whole-worm lysates in quadruplicate.

(E) Lifespan of N2 and *eat-2* worms subjected to RNAi-mediated KD of the TSP genes *cbs-1* or *cbl-1* as indicated.

(F) Lifespan analysis of WT or transgenic worms overexpressing CBS-1.

(G) Chronological lifespan of budding yeast grown in 2% or 0.5% glucose as indicated.

(H) H_2S production in yeast cultures grown in 2% or 0.5% glucose as detected by black lead sulfide accumulation on lead acetate papers inserted into the caps of the growth flasks and removed at the indicated time point.

(I) Schematic of transmethylation, TSP, and H_2S production in budding yeast.

(J) H_2S production in WT and sulfur assimilatory pathway mutant strains grown in 2% or 0.5% glucose for the indicated time.

(K) H_2S production in the met14 sulfur assimilatory mutant grown in 0.5% glucose and the indicated relative amount of Met or Cys.

(L) Chronological lifespan in 2% glucose ± H_2S donors NaHS and GYY4137 added during early culture growth at indicated time points (arrows).

All error bars SEM. See also Figure S6.

glucose-restricted cultures was detected within 24–48 hr and continued to increase for up to 96 hr in three different yeast strains (Figure 6H; Figures S6F and S6G). As the majority of H_2S production in yeast occurs via an assimilatory pathway not present in metazoans in which extracellular sulfate is converted to sulfide by the combined enzymatic activities of MET14, MET16, and MET5/10 (Figure 6I), we next asked if increased H_2S upon DR occurred through this assimilatory pathway or the conserved TSP pathway in yeast. Deletion of MET5, 14, or 16 resulted in inhibition of H_2S production under 2.0% glucose but did not block H_2S induction (Figure 6J) or chronological longevity extension (Figure S6H) upon glucose restriction. To further confirm Met and/or Cys, rather than inorganic sulfur, as the primary source of increased H_2S under conditions

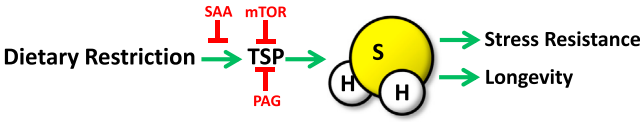

Figure 7. Model of DR-Mediated Benefits through Increased H_2S Production

DR regimens leading to extended longevity across evolutionary boundaries include PR, SAA restriction, and Cys restriction, leading to increased TSP activity via CGL and/or CBS family members, and increased endogenous H_2S production. Specific SAA addition, increased activity of the nutrient/energy sensing kinase, mechanistic target of rapamycin (mTOR), or the pharmacological agent, PAG, can block TSP upregulation and H_2S production. H_2S can readily diffuse through tissues and has pleiotropic, overlapping beneficial effects on the cellular, tissue, and organismal levels with the potential to contribute to stress resistance and longevity benefits of DR.

upon glucose restriction, we examined H_2S production in a Δmet14 line lacking a functional assimilatory pathway, with differing concentrations of Met and Cys in the media. Complete deprivation of either Met or Cys resulted in reduced H_2S production (Figure 6K). Thus, under conditions of glucose restriction, H_2S is produced from SAAs via the TSP. Because TSP-deficient CGL/STR1 and CBS/STR4 deletion strains grow abnormally in culture, it was not possible to test their requirement for increased H_2S production or extended chronological longevity under low-glucose conditions. However, exogenous H_2S donors NaHS and GYY4137 added early after inoculation were sufficient to significantly increase chronological lifespan (Figure 6L).

DISCUSSION

H_2S as Unifying Mechanism of DR Regimens and Benefits

As presented in the model in Figure 7, multiple DR regimens, including total food restriction, PR and SAA restriction/MetR, confer overlapping functional benefits in a number of diverse organisms from yeast (Johnson and Johnson, 2014) to worms (Cabreiro et al., 2013) to flies (Grandison et al., 2009; Troen et al., 2007) to rodents (Miller et al., 2005; Orentreich et al., 1993). In each of these experimental organisms, we found an increase in TSP-mediated H_2S production upon application of species-appropriate longevity regimens, ranging from EOD and MetR in mice to glucose restriction in yeast. Furthermore, in rodents and worms we demonstrated that genetic repression of TSP components blocked DR benefits, whereas overexpression could mimic benefits in the absence of any dietary intervention. In yeast, we found the TSP, rather than the assimilatory pathway, to be a major source of H_2S production upon glucose restriction. Although future studies are required to directly demonstrate the necessity of H_2S production for various DR benefits, our data demonstrate increased H_2S production via the TSP is an evolutionarily conserved response to DR from yeast to mammals with the potential to mediate multiple DR benefits including stress resistance and longevity. We note that the ability of SAA restriction to confer benefits in no way rules out other dietary triggers or downstream mechanisms of DR benefits, and that future studies will be required to determine if benefits attributed to different DR regimens, including Trp restriction, impact the TSP or H_2S production.

Regulation of TSP Gene Expression and H_2S Production

Cys deprivation triggers increased TSP gene expression possibly via the integrated stress response through GCN2 activation, eIF2α phosphorylation, and ATF4 stabilization (Lee et al., 2008). We confirmed the ability of DR to increase hepatic CGL expression in vivo, and Cys or NAC addback to block this induction. Whether or not GCN2 is required for this remains to be determined; however, our data suggest a role for mTORC1 in CGL regulation, because constitutive mTORC1 expression in the TSC1KO livers blocked diet-induced CGL expression.

Because the logic underlying TSP activation upon Cys deprivation is presumably to increase Cys biosynthesis, the notion that Cys degradation into H_2S increases when Cys concentrations are limiting is potentially counterintuitive. However, the in vivo source and identity of substrates for CGL or CBS-derived H_2S upon DR are not known. Free Cys released upon autophagy, rather than that produced de novo by TSP, could be a major fuel source for H_2S production. Interestingly, the benefits of MetR on longevity in yeast require autophagy (Ruckenstuhl et al., 2014), but whether autophagy plays a role in H_2S production remains to be determined.

Potential Mechanisms of H_2S Action in DR

By what mechanism(s) could endogenous H_2S give rise to pleiotropic DR benefits? We found that resistance to simulated IRI in vitro required the mitochondrial ETC component SQR. The SQR is thought to be of eubacterial origin and conserved from the early evolution of eukaryotes in an anoxic and sulfidic world (Theissen et al., 2003). H_2S could interact with SQR to lend protection against ischemia by donating electrons to the ETC via coenzyme Q, thus potentially serving as a source of electrons during ischemia. Interestingly, thiosulfate generated as a product of H_2S oxidation via SQR can undergo further chemical modification in a thioredoxin-reductase-dependent reaction using glutathione to produce sulfite and/or sulfate (Olson et al., 2013), which are used in some unicellular organisms as terminal electron acceptors for ATP production instead of oxygen, resulting in H_2S generation (Muyzer and Stams, 2008). Whether this can occur in mammalian cells remains to be explored; however, the addition of thiosulfate to hypoxic mammalian tissues results in the production of H_2S by unknown mechanisms (Olson et al., 2013).

Vasodilatory effects of H_2S could contribute to healthspan and lifespan extension in mammals by counteracting atherosclerosis, hypertension, and trauma. Exogenous H_2S protects the vasculature from oxidative damage (Yan et al., 2006), whereas a lack of CGL and/or endogenous H_2S production leads to hypertension (Yang et al., 2008). Fasting and PR protect the vasculature against intimal hyperplasia as a result of carotid focal stenosis (Mauro et al., 2014), correlating with increased H_2S production capacity upon DR in the carotid artery in vivo and vascular smooth muscle cells in vitro. Fasting protects the brain against IRI in rat models of transient middle cerebral artery occlusion (Varendi et al., 2014) and increased H_2S production capacity in mouse brain (Figure S6D). Future studies are required to address the specific role of increased TSP activity and H_2S

production in DR-mediated effects on the vasculature and other organ systems.

Clinical Significance

The use of exogenous H_2S as a DR mimetic is appealing for applications in which patient compliance with restricted food intake is an issue, but nonetheless remains challenging due to the short half-life of the gas in vivo and risks of toxicity at high levels. Modulation of endogenous H_2S production by diet offers advantages in terms of safety and continuous delivery in planned applications with brief duration, for example, in the context of preconditioning prior to elective surgery. In this context, H_2S may have pleiotropic advantages on surgical outcome, including vasodilatory and anti-inflammatory effects on the systemic level, as well as benefits against ischemic injury that may arise as part of the procedure itself or an unintended complication including heart attack or stroke.

Conclusions

H_2S was in vogue for centuries past as a cure-all before being viewed as a poisonous toxin with little or no acceptable level of exposure. Recently, H_2S has re-emerged as a potential therapeutic agent addressing numerous health issues (Zhang et al., 2013). Here, we identified DR as a trigger of increased endogenous H_2S production, and H_2S as a molecular mediator of pleiotropic DR benefits including longevity and stress resistance. These findings have broad implications for our basic understanding of DR and its potential clinical applications.

EXPERIMENTAL PROCEDURES

Additional details are provided in the Extended Experimental Procedures.

Mice

All experiments were performed with the approval of the Harvard Medical Area Animal Care and Use Committee (IACUC). Eight- to 10-week-old male B6D2F1 hybrids (The Jackson Laboratory) were used for all experiments unless otherwise indicated. Male and female NRF2 KO and littermate controls on a mixed 129/C57BL/6 background (Martin et al., 1998), LTsc1KO and littermate controls on a C57BL/6 background (Harputlugil et al., 2014), and CGLKO and control mice on a mixed 129/C57BL/6 background (Yang et al., 2008) were described previously.

Preconditioning Regimens

Dietary

Mice were given AL access to food and water unless otherwise indicated. Experimental diets were based on Research Diets D12450B with approximately 18% of calories from protein (hydrolyzed casein or individual crystalline amino acids [Ajinomoto] in the proportions present in casein), 10% from fat and 72% from carbohydrate. AL food intake was monitored for several days and used to calculate 50% DR. Mice were fed daily with fresh food between 6 and 7 p.m.

Pharmacological

NAC (600 mg/kg/day total in food and drinking water) and VitC&E (1,000 and 250 mg/kg/day, respectively, in food and drinking water) supplementation was halted 16–24 hr prior to organ harvest and/or induction of IRI. NaHS (1 mM) or GYY4137 (260 μM final) was delivered in the drinking water; PAG (10 mg/kg) and NaHS (3–5 mg/kg) were administered by IP injection.

Adenoviral-Mediated Gene Delivery

CGL was overexpressed by intravenous injection of 10^{10} plaque-forming units of Ad-CMV-CGL (ADV-256305) or control Ad-CMV Null virus (Vector Biolabs) 7 days prior to hepatic IRI.

Cells

In vitro DR was performed in mouse Hepa1-6 cells, primary hepatocytes, or primary aortic smooth muscle cells by incubating in DMEM lacking Met and Cys (Invitrogen) with 10% dialyzed FBS for up to 20 hr.

Ischemia Reperfusion Models

In Vivo

Warm hepatic or renal IRI was induced, and damage was assessed as previously described (Peng et al., 2012). ALT, AST, and/or LDH values were normalized to the experimental control; usually the WT group fed a complete diet AL, for each time point (3, 24 hr postreperfusion) and combined into a single value per animal.

In Vitro

For simulated ischemia, growth or preconditioning media was replaced with saline to mimic nutrient/energy deprivation and placed in an airtight chamber flushed with nitrogen gas at 37°C for 4 hr. Saline supernatant was removed after simulated ischemia for LDH measurement. Reperfusion was simulated by adding back fresh complete DMEM-12320 (Invitrogen) containing 0.5 mg/ml MTT under normoxia at 37°C for an additional 3–4 hr.

Metabolic Parameters

Body composition was determined with an Echo MRI. Blood glucose was measured with an Easy Step Glucometer (Home Aide Diagnostics), serum triglycerides with a Serum Triglyceride Determination Kit (Sigma), liver RONS and GSH from left hepatic lobes normalized by wet weight using OxiSelect In Vitro Green Fluorescence ROS/RNS Assay Kit (Cell Biolabs) and the fluorimetric Glutathione Assay Kit (Sigma), and liver metabolites via mass spectrometry and normalized to total protein content. Peroxisome β-oxidation of lipids was performed on freshly harvested liver (Hu et al., 2005; Lazarow, 1981).

mRNA and Protein Analysis

Total RNA was isolated from tissues and cells using miRNeasy Mini Kit (QIAGEN) and cDNA synthesized by random hexamer priming with the Verso cDNA kit (Thermo Scientific). qRT-PCR was performed with SYBR green dye (Lonza) and TaqPro DNA polymerase (Denville). Fold changes were calculated by the $\Delta\Delta C_t$ method using Hprt and/or Rpl13 as standards and normalized to the experimental WT AL control. Protein expression was analyzed in tissues homogenized in passive lysis buffer (Promega), separated by SDS-PAGE, transferred to PVDF membrane (Whatman), and blotted for CGL (ab151769 Abcam), CBS (ab135626 Abcam), or actin (13E5 Cell Signaling) followed by HPRT-conjugated secondary anti-rabbit antibody (Dako).

H_2S Measurements

Lead Sulfide Method

H_2S production capacity was measured in 100 mg fresh tissue or 100–300 μg freeze-thaw homogenate in passive lysis buffer (Promega) of tissues, flies or worms, in PBS supplemented with 10 mM Cys and 10 μM-6 mM PLP. A lead acetate H_2S detection paper (Sigma; or made by soaking blotting paper [VWR] in 20 mM lead acetate [Sigma] and then vacuum drying) was placed above the liquid phase in a closed container (microcentrifuge tube or covered 96-well plate) and incubated 2–5 hr at 37°C until lead sulfide darkening of the paper occurred. In live Hepa1-6 cells in 96-well plates, growth media was supplemented with 10 mM Cys and 10 μM PLP, and a lead acetate paper placed over the plate for 2–24 hr of further incubation in a CO_2 incubator at 37°C. In live yeast culture, lead acetate papers were placed above liquid cultures at the time of inoculation.

Sulfide Probe Method

A microsulfide ion electrode probe (Lazar Research Laboratories) and volt meter (Jenco) were used to measure H_2S production capacity in extracts in vitro and endogenous H_2S concentrations in liver in vivo upon direct insertion into median and left lobes of anesthetized mice prior to sacrifice.

Fly Conditions

D. melanogaster were maintained as described previously (Lee et al., 2014). Flies used in the H_2S production capacity assay were held on the designated diet and transferred to fresh vials without anesthesia every 3 days until 18 days of age.

Worm Conditions

N2 and DA1116 (*eat-2(ad1116)* II.) strains were grown following standard procedures, and all lifespan experiments were carried out as previously described (Mair et al., 2011). RNAi clones were from the Ahringer RNAi library. CBS transgenic strains overexpressing the *cbs-1* isoform a (ZC373.1a) from the ubiquitous *sur-5* promoter and *unc-54* 3′ UTR were generated by microinjection into gonads of young adult hermaphrodites.

Yeast Conditions

Experiments were carried out in WT strains BY4742 (MATα his3Δ1 leu2Δ0 lys2Δ0 ura3Δ0), W303 (MATa leu2-3,112 trp1-1 can1-100 ura3-1 ade2-1 his3-11,15), and DBY746 (MATα leu2-3, 112 his3Δ1 trp1-289 ura 3-52 GAL^+). Met deletion strains in BY4742 (met5, met14, and met16) were purchased from EUROSCARF. For chronological aging experiments, cells were inoculated to an OD_{600} of 0.05 and grown at 28°C in SCD media, and cell survival was determined by clonogenicity at the given time points in at least three independent cultures, and values were normalized to survival on day 1. Longevity effects of exogenous H_2S were tested by adding 100 μM GYY4137 (in DMSO) to BY4742 cultures at the time of inoculation and 5 μM NaHS at 6, 24, and 48 hr after inoculation, with DMSO-treated BY4742 as a control.

Statistical Analyses

Data are displayed as means ± SEM, and statistical significance was assessed in GraphPad Prism using Student's t tests to compare values and one-sample t test to compare means to a hypothetical value of 1 or 100 when data were normalized to the average value of the control group. A p value of 0.05 or less was deemed statistically significant.

SUPPLEMENTAL INFORMATION

Supplemental Information includes Extended Experimental Procedures and six figures and can be found with this article online at http://dx.doi.org/10.1016/j.cell.2014.11.048.

ACKNOWLEDGMENTS

We thank Bruce Kristal and Jaan-Olle Andressoo for critical reading of the manuscript; Silvia Dichtinger, Manmeet Gujral, and Jason Li for technical assistance; and Paul Ney for sharing the NRF2KO mice. This work was supported by grants from NIH (RO1DK090629, R01AG036712) and the Glenn Foundation to J.R.M.; C.H. was supported by T32CA0093823; F.M. was supported by the Austrian Science Fund FWF (LIPOTOX, I1000, P23490-B12, and P24381-B20); W.B.M. was supported by 1R01AG044346; V.N.G. was supported by R01AG021518; C.K.O. was supported by American Heart Association 12GRNT9510001 and 12GRNT1207025; and R.W. was supported by an operating grant from the Canadian Institutes of Health Research.

Received: April 1, 2014
Revised: September 12, 2014
Accepted: November 18, 2014
Published: December 23, 2014

REFERENCES

Bishop, N.A., and Guarente, L. (2007). Two neurons mediate diet-restriction-induced longevity in C. elegans. Nature *447*, 545–549.

Blackstone, E., Morrison, M., and Roth, M.B. (2005). H2S induces a suspended animation-like state in mice. Science *308*, 518.

Cabreiro, F., Au, C., Leung, K.Y., Vergara-Irigaray, N., Cochemé, H.M., Noori, T., Weinkove, D., Schuster, E., Greene, N.D., and Gems, D. (2013). Metformin retards aging in C. elegans by altering microbial folate and methionine metabolism. Cell *153*, 228–239.

Calabrese, E.J., and Mattson, M.P. (2011). Hormesis provides a generalized quantitative estimate of biological plasticity. J. Cell Commun. Signal. *5*, 25–38.

Calvert, J.W., Coetzee, W.A., and Lefer, D.J. (2010). Novel insights into hydrogen sulfide—mediated cytoprotection. Antioxid. Redox Signal. *12*, 1203–1217.

Cuevasanta, E., Denicola, A., Alvarez, B., and Möller, M.N. (2012). Solubility and permeation of hydrogen sulfide in lipid membranes. PLoS ONE *7*, e34562.

Fontana, L., Partridge, L., and Longo, V.D. (2010). Extending healthy life span—from yeast to humans. Science *328*, 321–326.

Grandison, R.C., Piper, M.D., and Partridge, L. (2009). Amino-acid imbalance explains extension of lifespan by dietary restriction in Drosophila. Nature *462*, 1061–1064.

Harputlugil, E., Hine, C., Vargas, D., Robertson, L., Manning, B.D., and Mitchell, J.R. (2014). The TSC complex is required for the benefits of dietary protein restriction on stress resistance in vivo. Cell Reports *8*, 1160–1170.

Hildebrandt, T.M., and Grieshaber, M.K. (2008). Three enzymatic activities catalyze the oxidation of sulfide to thiosulfate in mammalian and invertebrate mitochondria. FEBS J. *275*, 3352–3361.

Hine, C.M., and Mitchell, J.R. (2012). NRF2 and the phase II response in acute stress resistance induced by dietary restriction. J Clin Exp Pathol *S4*.

Hu, T., Foxworthy, P., Siesky, A., Ficorilli, J.V., Gao, H., Li, S., Christe, M., Ryan, T., Cao, G., Eacho, P., et al. (2005). Hepatic peroxisomal fatty acid beta-oxidation is regulated by liver X receptor alpha. Endocrinology *146*, 5380–5387.

Johnson, J.E., and Johnson, F.B. (2014). Methionine restriction activates the retrograde response and confers both stress tolerance and lifespan extension to yeast, mouse and human cells. PLoS ONE *9*, e97729.

Kabil, H., Kabil, O., Banerjee, R., Harshman, L.G., and Pletcher, S.D. (2011a). Increased transsulfuration mediates longevity and dietary restriction in Drosophila. Proc. Natl. Acad. Sci. USA *108*, 16831–16836.

Kabil, O., Vitvitsky, V., Xie, P., and Banerjee, R. (2011b). The quantitative significance of the transsulfuration enzymes for H2S production in murine tissues. Antioxid. Redox Signal. *15*, 363–372.

Kang, K., Zhao, M., Jiang, H., Tan, G., Pan, S., and Sun, X. (2009). Role of hydrogen sulfide in hepatic ischemia-reperfusion-induced injury in rats. Liver Transpl. *15*, 1306–1314.

Lakowski, B., and Hekimi, S. (1998). The genetics of caloric restriction in Caenorhabditis elegans. Proc. Natl. Acad. Sci. USA *95*, 13091–13096.

Lazarow, P.B. (1981). Assay of peroxisomal beta-oxidation of fatty acids. Methods Enzymol. *72*, 315–319.

Lee, J.I., Dominy, J.E., Jr., Sikalidis, A.K., Hirschberger, L.L., Wang, W., and Stipanuk, M.H. (2008). HepG2/C3A cells respond to cysteine deprivation by induction of the amino acid deprivation/integrated stress response pathway. Physiol. Genomics *33*, 218–229.

Lee, Z.W., Zhou, J., Chen, C.S., Zhao, Y., Tan, C.H., Li, L., Moore, P.K., and Deng, L.W. (2011). The slow-releasing hydrogen sulfide donor, GYY4137, exhibits novel anti-cancer effects in vitro and in vivo. PLoS ONE *6*, e21077.

Lee, B.C., Kaya, A., Ma, S., Kim, G., Gerashchenko, M.V., Yim, S.H., Hu, Z., Harshman, L.G., and Gladyshev, V.N. (2014). Methionine restriction extends lifespan of Drosophila melanogaster under conditions of low amino-acid status. Nat. Commun. *5*, 3592.

Levine, M.E., Suarez, J.A., Brandhorst, S., Balasubramanian, P., Cheng, C.W., Madia, F., Fontana, L., Mirisola, M.G., Guevara-Aguirre, J., Wan, J., et al. (2014). Low protein intake is associated with a major reduction in IGF-1, cancer, and overall mortality in the 65 and younger but not older population. Cell Metab. *19*, 407–417.

Liu, M., Grigoryev, D.N., Crow, M.T., Haas, M., Yamamoto, M., Reddy, S.P., and Rabb, H. (2009). Transcription factor Nrf2 is protective during ischemic and nephrotoxic acute kidney injury in mice. Kidney Int. *76*, 277–285.

Mair, W., Morantte, I., Rodrigues, A.P., Manning, G., Montminy, M., Shaw, R.J., and Dillin, A. (2011). Lifespan extension induced by AMPK and calcineurin is mediated by CRTC-1 and CREB. Nature *470*, 404–408.

Martin, F., van Deursen, J.M., Shivdasani, R.A., Jackson, C.W., Troutman, A.G., and Ney, P.A. (1998). Erythroid maturation and globin gene expression in mice with combined deficiency of NF-E2 and nrf-2. Blood *91*, 3459–3466.

Mauro, C.R., Tao, M., Yu, P., Treviño-Villerreal, J.H., Longchamp, A., Kristal, B.S., Ozaki, C.K., and Mitchell, J.R. (2014). Preoperative dietary restriction

reduces intimal hyperplasia and protects from ischemia-reperfusion injury. J. Vasc. Surg.

Miller, D.L., and Roth, M.B. (2007). Hydrogen sulfide increases thermotolerance and lifespan in Caenorhabditis elegans. Proc. Natl. Acad. Sci. USA *104*, 20618–20622.

Miller, R.A., Buehner, G., Chang, Y., Harper, J.M., Sigler, R., and Smith-Wheelock, M. (2005). Methionine-deficient diet extends mouse lifespan, slows immune and lens aging, alters glucose, T4, IGF-I and insulin levels, and increases hepatocyte MIF levels and stress resistance. Aging Cell *4*, 119–125.

Mitchell, J.R., Verweij, M., Brand, K., van de Ven, M., Goemaere, N., van den Engel, S., Chu, T., Forrer, F., Müller, C., de Jong, M., et al. (2010). Short-term dietary restriction and fasting precondition against ischemia reperfusion injury in mice. Aging Cell *9*, 40–53.

Módis, K., Coletta, C., Erdélyi, K., Papapetropoulos, A., and Szabo, C. (2013). Intramitochondrial hydrogen sulfide production by 3-mercaptopyruvate sulfurtransferase maintains mitochondrial electron flow and supports cellular bioenergetics. FASEB J. *27*, 601–611.

Muyzer, G., and Stams, A.J. (2008). The ecology and biotechnology of sulphate-reducing bacteria. Nat. Rev. Microbiol. *6*, 441–454.

Olson, K.R., Deleon, E.R., Gao, Y., Hurley, K., Sadauskas, V., Batz, C., and Stoy, G.F. (2013). Thiosulfate: a readily accessible source of hydrogen sulfide in oxygen sensing. Am. J. Physiol. Regul. Integr. Comp. Physiol. *305*, R592–R603.

Orentreich, N., Matias, J.R., DeFelice, A., and Zimmerman, J.A. (1993). Low methionine ingestion by rats extends life span. J. Nutr. *123*, 269–274.

Paul, B.D., and Snyder, S.H. (2012). H_2S signalling through protein sulfhydration and beyond. Nat. Rev. Mol. Cell Biol. *13*, 499–507.

Pearson, K.J., Lewis, K.N., Price, N.L., Chang, J.W., Perez, E., Cascajo, M.V., Tamashiro, K.L., Poosala, S., Csiszar, A., Ungvari, Z., et al. (2008). Nrf2 mediates cancer protection but not prolongevity induced by caloric restriction. Proc. Natl. Acad. Sci. USA *105*, 2325–2330.

Peng, W., Robertson, L., Gallinetti, J., Mejia, P., Vose, S., Charlip, A., Chu, T., and Mitchell, J.R. (2012). Surgical stress resistance induced by single amino Acid deprivation requires gcn2 in mice. Sci. Transl. Med. *4*, 118ra111.

Predmore, B.L., Alendy, M.J., Ahmed, K.I., Leeuwenburgh, C., and Julian, D. (2010). The hydrogen sulfide signaling system: changes during aging and the benefits of caloric restriction. Age (Dordr.) *32*, 467–481.

Ristow, M., and Schmeisser, S. (2011). Extending life span by increasing oxidative stress. Free Radic. Biol. Med. *51*, 327–336.

Ruckenstuhl, C., Netzberger, C., Entfellner, I., Carmona-Gutierrez, D., Kickenweiz, T., Stekovic, S., Gleixner, C., Schmid, C., Klug, L., Sorgo, A.G., et al. (2014). Lifespan extension by methionine restriction requires autophagy-dependent vacuolar acidification. PLoS Genet. *10*, e1004347.

Sinclair, D.A. (2005). Toward a unified theory of caloric restriction and longevity regulation. Mech. Ageing Dev. *126*, 987–1002.

Stipanuk, M.H., and Ueki, I. (2011). Dealing with methionine/homocysteine sulfur: cysteine metabolism to taurine and inorganic sulfur. J. Inherit. Metab. Dis. *34*, 17–32.

Tapia, P.C. (2006). Sublethal mitochondrial stress with an attendant stoichiometric augmentation of reactive oxygen species may precipitate many of the beneficial alterations in cellular physiology produced by caloric restriction, intermittent fasting, exercise and dietary phytonutrients: ''Mitohormesis'' for health and vitality. Med. Hypotheses *66*, 832–843.

Theissen, U., Hoffmeister, M., Grieshaber, M., and Martin, W. (2003). Single eubacterial origin of eukaryotic sulfide:quinone oxidoreductase, a mitochondrial enzyme conserved from the early evolution of eukaryotes during anoxic and sulfidic times. Mol. Biol. Evol. *20*, 1564–1574.

Troen, A.M., French, E.E., Roberts, J.F., Selhub, J., Ordovas, J.M., Parnell, L.D., and Lai, C.Q. (2007). Lifespan modification by glucose and methionine in Drosophila melanogaster fed a chemically defined diet. Age (Dordr.) *29*, 29–39.

Varendi, K., Airavaara, M., Anttila, J., Vose, S., Planken, A., Saarma, M., Mitchell, J.R., and Andressoo, J.O. (2014). Short-term preoperative dietary restriction is neuroprotective in a rat focal stroke model. PLoS ONE *9*, e93911.

Wu, Z., Liu, S.Q., and Huang, D. (2013). Dietary restriction depends on nutrient composition to extend chronological lifespan in budding yeast Saccharomyces cerevisiae. PLoS ONE *8*, e64448.

Yan, S.K., Chang, T., Wang, H., Wu, L., Wang, R., and Meng, Q.H. (2006). Effects of hydrogen sulfide on homocysteine-induced oxidative stress in vascular smooth muscle cells. Biochem. Biophys. Res. Commun. *351*, 485–491.

Yang, G., Wu, L., Jiang, B., Yang, W., Qi, J., Cao, K., Meng, Q., Mustafa, A.K., Mu, W., Zhang, S., et al. (2008). H2S as a physiologic vasorelaxant: hypertension in mice with deletion of cystathionine gamma-lyase. Science *322*, 587–590.

Zhang, Y., Tang, Z.H., Ren, Z., Qu, S.L., Liu, M.H., Liu, L.S., and Jiang, Z.S. (2013). Hydrogen sulfide, the next potent preventive and therapeutic agent in aging and age-associated diseases. Mol. Cell. Biol. *33*, 1104–1113.

Cell

EXTENDED EXPERIMENTAL PROCEDURES

Mice

All rodent experiments were performed with the approval of the appropriate institutional animal care and use committee. Male B6D2F1 hybrid mice 8-10 weeks of age purchased from The Jackson Laboratory were used for all experiments unless otherwise indicated. Male and female NRF2 KO and littermate control mice on a mixed 129/C57BL6 background generated previously (Martin et al., 1998) were bred in our facility and used at the age of 8-10 weeks. LTsc1KO and littermate control animals were generated by crossing $Tsc1^{fl/fl}$ (WT) mice with $Tsc1^{fl/fl}$ | Albumin-Cre+/− (LTsc1KO) mice as previously described (Harputlugil et al., 2014). 8 week old male CGL WT and KO mice were generated as previously described (Yang et al., 2008).

Preconditioning Regimens

Dietary

Mice were given *ad libitum* (AL) access to food and water unless otherwise indicated. Experimental diets were based on Research Diets D12450B with approximately 18% of calories from protein (hydrolyzed casein or individual crystalline amino acids (Ajinomoto) in the proportions present in casein), 10% from fat and 72% from carbohydrate. AL food intake per gram of body weight was monitored daily for several days and used to calculate 50% dietary restriction (DR) based on initial animal weights. Protein free diets were kept isocaloric by replacing casein/amino acids with an equal weight of sucrose and provided either AL or 35% DR as indicated. MetR diets containing 1.5g Met/kg food and lacking Cys (Miller et al., 2005) were provided AL. Met and Cys supplementation back to AL levels in DR diets was achieved by raising Met content from 2.5 to 5g/kg of food, and Cys content from 2 to 4g/kg food. Animals were fed daily with fresh food between 6pm and 7pm.

Pharmacological

NAC was supplemented at a daily dose of ~600mg/kg/day, with ~400mg/kg/day in the food and ~200mg/kg/day in the drinking water (Parnell et al., 2010). Antioxidant vitamins were supplemented in the food at 1000 mg/kg/day VitC (Ergul et al., 2010) and 250 mg/kg/day VitE (Calfee-Mason et al., 2002). NAC and VitC&E supplementation was halted 16-24 hr prior to organ harvest and/or induction of IRI. NaHS (1mM final) or GYY4137 (260 μM final) were placed in the drinking water 7 days prior to hepatic IRI with fresh water changes occurring every day for NaHS and on day 3 for GYY4137. PAG (10mg/kg in saline) and NaHS (3-5mg/kg in saline) were administered by IP injection.

Adenoviral-Mediated Gene Delivery

Overexpression of CGL was accomplished by IV injection of 10^{10} PFUs of an adenovirus-type 5 (dE1/E3) containing the CMV promoter driving expression of the mouse CGL gene (Ad-mCTH/CGL, GenBank RefSeq BC019483, ADV-256305 Vector Biolabs) or the negative control virus Ad-CMV Null (1300 Vector Biolabs) 7-days prior to hepatic IRI.

IRI and Measurements of Damage

Warm hepatic or renal ischemia reperfusion injury was induced as previously described (Peng et al., 2012). Briefly, mice were anesthetized with isoflurane and body temperature maintained on a circulating heated water pad. Following laparotomy, a microvascular clamp (Roboz) was placed over the portal triad for hepatic ischemia for 35min, or over each renal pedicle for bilateral renal ischemia for 30min, followed by clamp removal and wound closure. Serum was collected from small volumes of tail blood for up to 24hrs after hepatic injury and up to 48hrs after renal injury. Liver damage was assessed by kinetic measurements of serum ALT, AST (Infinity Reagents, Thermo Scientific) and LDH (Pointe Scientific) in a microtiter plate reader (Biotek Synegy2) and confirmed on a different platform (Piccolo Liver Plus discs, Abaxis). Data for ALT, AST, and/or LDH were normalized to the experimental control for each time point, usually the AL WT group, and time points post reperfusion were combined into one value of liver damage per animal. 24 hr post reperfusion, the left liver lobe was harvested and formalin fixed. Images were taken via digital camera and shown at 1x magnification. Fixed lobes were then paraffin embedded, cut into sections and stained with hematoxylin and eosin for confirmation of liver damage. Representative images are shown with 250 μm scale bars.

Metabolic Parameters

Mouse weights and % fat mass were obtained using an electronic scale and live animal MRI-based body composition analysis (Echo MRI). Blood glucose was measured from fresh tail blood with an Easy Step Glucometer (Home Aide Diagnostics). True serum triglycerides were calculated from measurements of free glycerol and total glycerol after lipolysis using the Serum Triglyceride Determination Kit (Sigma). Liver RONS and GSH were analyzed from left hepatic lobes normalized by wet weight using OxiSelect In Vitro Green Fluorescence ROS/RNS Assay Kit (Cell Biolabs) and the fluorimetric Glutathione Assay Kit (Sigma) according to the manufacture's recommendations. Peroxisome β-oxidation of lipids was performed on freshly harvested liver (Hu et al., 2005; Lazarow, 1981). Briefly, 100mg of liver was placed into 900uL of ice-cold 0.25M sucrose, homogenized on ice, and centrifuged at 600 g for 10min. 450uL of was mixed with 50uL of 10% Triton X-100 (Sigma) on ice, from which 5uL was mixed with 200uL of reaction mix in a 96-well plate and incubated at 37°C for one minute followed by ± addition of 2uL of palmitoyl-CoA. Peroxisomal lipid oxidation was proportional to the rate of NADH formation in the presence of cyanide to block mitochondrial NADH oxidation. Liver metabolites normalized to total protein content were measured via mass spectrometry at the Beth Israel Deaconess Medical Center Core Facility.

Gene Expression Analysis by qPCR and Western Blot

Total RNA was isolated from tissues and cells using miRNeasy Mini Kit (QIAGEN) and cDNA synthesized by random hexamer priming with the Verso cDNA kit (Thermo). qRT-PCR was performed with SYBR green dye (Lonza) and TaqPro DNA polymerase (Denville). Fold changes were calculated by the $\Delta\Delta C_t$ method using Hprt and/or Rpl13 genes as standards, and normalized to the experimental WT AL control. Primer sequences are as follows:

CGL For: TTGGATCGAAACACCCACAAA Rev: AGCCGACTATTGAGGTCATCA; CBS For: GGGACAAGGATCGAGTCTGGA Rev: AGCACTGTGTGATAATGTGGG; HO-1 For: AAGCCGAGAATGCTGAGTTCA Rev: GCCGTGTAGATATGGTACAAGGA; NQO-1 For: AGGATGGGAGGTACTCGAATC Rev: AGGCGTCCTTCCTTATATGCTA; GSTA4 For: TGATTGCCGTGGCTCCATTTA Rev: CAACGA GAAAAGCCTCTCCGT; GSTM4 For: AGCTCACGCTATTCGGCTG Rev: GCTCCAAGTATTCCACCTTCAGT; GSTT3 For: GGATGGG GACTTCGTCTTGG Rev: TCAGGAGGTACGGGCTGTC; LCAD For: TCTTTTCCTCGGAGCATGACA Rev: GACCTCTCTACTCACTT CTCCAG; Cyp4a14 For: TTTAGCCCTACAAGGTACTTGGA Rev: GCAGCCACTGCCTTCGTAA; HPRT For: TTTCCCTGGTTAAG CAGTACAGCCC Rev: TGGCCTGTATCCAACACTTCGAGA; RPL13 For: TTCGGCTGAAGCCTACCAGAAAGT Rev: TCTTCCGATAG TGCATCTTGGCCT; SOD1 For: GGGACAATACACAAGGCTGT Rev: GCCAATGATGGAATGCTCTC; SOD2 For: GCTTGGCTTCAA TAAGGAGC Rev: TGAAGGTAGTAAGCGTGCTC; Catalase For: CGGTAGCTGTGAACTGTCCCTACCG Rev: CTCTGGTGCGCT GAAGCTGT.

For protein expression analysis, tissues were homogenized with passive lysis buffer (Promega), normalized for protein content, boiled with SDS loading buffer and separated by SDS-PAGE. Proteins were transferred to PVDF membrane (Whatman) and blotted for CGL (ab151769 Abcam), CBS (ab135626 Abcam) and Actin (13E5 Cell Signaling) and secondarily with HPRT conjugated anti-rabbit antibody (Dako).

H_2S Measurements

Lead Sulfide Method on Intact Tissues

For detection of H_2S production capacity from intact fresh tissue, 100mg of fresh liver and/or kidney tissue was placed in a 1.5mL centrifuge tube containing 750 μl of 10mM Cys (Sigma) and 10 μM Pyridoxal 5′-phosphate (PLP) (Sigma) in PBS. A rectangular lead acetate H_2S detection strip (Sigma) was wedged into the lid of the microcentrifuge tube so as to avoid contact with the supernatant. Closed tubes were incubated 2-5 hr at 37°C until visible, but not oversaturated, lead sulfide darkening of the paper occurred.

Lead Sulfide Method on Lysates or Live Cells

For detection of H_2S production capacity from homogenized tissues, flies or worms, samples were homogenized in passive lysis buffer (Promega) followed by several rounds of flash freezing/thawing. Protein content and volume were normalized via BCA Kit (Thermo). 100-300 μg of protein was added to a final reaction in 96-well format containing 10mM Cys and 10 μM PLP for mammalian tissue, 2mM for worm and 6mM for flies. 6x4 inch pieces of lead acetate paper, made by soaking 703 size blotting paper (VWR) in 20mM lead acetate (Sigma) and then vacuum drying, were placed over the 96-well dish and incubated for 2-24 hr at 37°C until lead sulfide was detected but not saturated. For detection of H_2S production in live Hepa1-6 cells grown in 96-well plates, growth media was supplemented with 10mM Cys and 10 μM PLP, and a lead acetate paper placed over the plate for 2-24 hr of further incubation in a CO_2 incubator at 37°C.

Lead Sulfide Method in Live Yeast Culture

Lead acetate paper squares were placed on the bottom of the flask stopper at the time of inoculation of yeast in media containing 2% or 0.5% glucose.

H_2S Detection with Microsulfide Probe

A micro-sulfide ion electrode probe (Lazar Research Laboratories) and volt meter (Jenco) were used to measure H_2S production capacity in extracts in vitro and endogenous hepatic H_2S levels in vivo. The probe was calibrated to a set of NaHS standards to obtain a trend line and equation needed to transform the mV readings into H_2S concentrations. For homogenized extracts in vitro, an equal amount of protein (100-300 μg) was added to a final reaction containing 10mM Cys and 10 μM PLP in a 96-well plate and covered with cellophane to isolate each well and trap any gas that was produced. After 3 hr of incubation, mV readings were taken after inserting the probe through the cellophane covering into each well individually. For in vivo measurements of endogenous H_2S concentrations, the probe was inserted directly into median and left liver lobes of anesthetized mice prior to sacrifice.

Simulated In Vitro DR

Hepa1-6 cells were cultured in complete RPMI-1640 (Sigma) supplemented with 10% FBS at 37°C in 20% O_2 until ~70%–80% confluence. Equal numbers of cells were then seeded into 96-well format in complete RPMI-1640. When cultures obtained ~70%–80% confluence, the media was removed and replaced either with complete RPMI-1640 or RPMI lacking Met and Cys (Sigma), both supplemented with 10% dialyzed FBS, and the cells incubated overnight for 16 hr.

Primary hepatocytes were isolated by collagenase treatment (Liberase, Roche), Percoll (GE Healthcare) gradient centrifugation and initially cultured in William's E media (Sigma) with 5% FBS for several hours. The media was then removed and replaced with complete or Met and Cys null DMEM-12320 media (Invitrogen) supplemented with 10% dialyzed FBS overnight for 16 hr.

Primary mouse aortic smooth muscle cells were prepared from thoracic aorta. Following dissection of periadventitial tissues under a dissecting microscope, the aorta was minced into small pieces and placed as explants, luminal side down, on the dry surface of a 24-well culture plate previously coated with 7% Cell-Tak (Corning). Explants were gently covered with one drop of RPMI, 10%FBS

medium, and placed overnight in a 37°C, 5% CO_2. The next day, culture medium was carefully added to the wells without detaching the explants. SMCs were identified by immunostaining using antibodies to smooth muscle actin (abcam, ab5694) and desmin (Dako, M 0760). Passages 1 to 4 were used for the experiments. For in vitro DR, complete media was removed and replaced with either complete or Met and Cys null DMEM (Invitrogen) for up to 20hrs prior to H_2S detection.

Simulated In Vitro Ischemia Reperfusion Injury and Oxidative Stress

Growth or preconditioning media was replaced with saline to mimic nutrient/energy deprivation, with or without NaHS (10 μM) or thiosulfate (1, 10, or 100 μM, Sigma). For hypoxia, plates were placed in an airtight chamber flushed with nitrogen gas at 37°C for 4hrs. At the end of the hypoxic period, the saline supernatant was removed and tested for cell damage (LDH release). Reperfusion was simulated by adding back fresh complete DMEM-12320 containing 0.5mg/mL MTT (Invitrogen) and incubating at normoxia at 37°C for an additional 3-4hrs. The media was removed and replaced with acid isopropanol (0.04M HCl in isopropanol) and absorbance read at 520nM or analyzed for LDH activity. H_2S-mediated protection from oxidative stress in Hepa1-6 or primary vascular smooth muscle cells was performed by adding 10 μM or 100 μM H_2S to the cell culture media prior to challenge with H_2O_2 at a final concentration of 5mM for Hepa1-6 and 1mM for smooth muscle cells 24hrs prior to analysis for LDH and MTT.

siRNA Knockdown In Vitro

siRNA knockdown of mouse Sulfide Quinone Oxidoreductase (SQR) was performed in Hepa1-6 cells as described previously (Módis et al., 2013) with the following siRNA oligos: Sense: GACGAGAACUGUAUCCGCAtt and AntiSense: UGCGGAUACAGUUCUC GUCtg, with RNA in uppercase and DNA in lowercase. Knockdown was confirmed by SQR immunoblot (ProteinTech).

Fly Conditions

D. melanogaster (Canton-S) line was from the laboratory of Dr. Lawrence G. Harshman (University of Nebraska, Lincoln, NE). Flies were maintained on corn meal food and kept in a temperature-controlled chamber at 25°C with 12hr light/dark cycle and approximately 60% humidity. Newly emerged flies were transferred to fresh corn meal food and allowed to mate for 1-2 days. Three day old mated flies were collected using CO_2, sorted by sex and then female flies were transferred to cages on the fully defined medium containing 62.08 g Diet TD.04310 (corresponds to the 0.1X diet) and/or 101.07 g Diet TD.10417 (corresponds to the 1.0X diet) (Harlan Teklad), 100mg lecithin from soybean (Sigma), 500 mg ribonucleic acid from Torula yeast (Sigma), 100 g of dextrose, 20 g agar, 2.85mL propionic acid, 0.255mL of phosphoric acid (Sigma), and indicated amounts of Met (Sigma) per liter of water. To prepare 0.4X and 0.7X diets, the two basal mixes were mixed to adjust amino acid concentrations (Lee et al., 2014). The experimental flies were held on the designed diet and transferred to fresh vials without anesthesia every three days. After 18 days, all flies were collected and then used for H_2S production assay.

Worm Conditions

N2 and DA1116 (*eat-2(ad1116)* II.) strains were grown on 6 cm nematode growth media plates following standard procedures. RNAi clones were from Ahringer RNAi library. RNAi bacterial cultures were grown overnight at 37°C in the presence of carbenicillin (100 μg/mL) and tetracycline (10 μg/mL) before seeding to NGM plates containing carbenicillin (100 μg/mL). Seeded RNAi plates were allowed to grow at room temperature for 48 hr. Expression of dsRNA was induced with 100 μl of IPTG (100 mM) 2 hr before worms were transferred to the plates. All lifespan experiments were carried out as previously described (Mair et al., 2011). In summary, worms were synchronized with a timed egg lay or bleach. Eggs were allowed to hatch and grow to adulthood on control or RNAi plates, respectively. Day 1 of lifespan assay was defined as the first day of adulthood. Worms were transferred to fresh RNAi plates and scored for death or censor events every 1-2 days until day 14, after which they were scored every 1-2 days but only transferred once per week. Death was scored as no response to gentle agitation at the head or tail. Those worms that died as a result of internal hatching or crawling off the plates were scored as censored. Transgenic *C. elegans* strain construction for CBS overexpression: *C. elegans cbs-1* isoform a (ZC373.1a) was PCR amplified and subsequently fused in-frame to the N terminus of tandem-dimer TOMATO. The fusion protein was expressed using the ubiquitous *sur-5* promoter and *unc-54* 3′ UTR. 50 ng/μl of the *cbs-1* construct was mixed with 50 ng/μl of pCFJ104 (*myo-3*p:mCherry) as co-injection marker and microinjected into gonads of hermaphrodites to generate transgenic strains.

Yeast Conditions

Experiments were carried out in wild-type strains BY4742 (MATα his3Δ1 leu2Δ0 lys2Δ0 ura3Δ0), W303 (MATa leu2-3,112 trp1-1 can1-100 ura3-1 ade2-1 his3-11,15), and DBY746 (MATα leu2-3, 112 his3Δ1 trp1-289 ura 3-52 GAL+) grown in SCD media. Met deletion strains in BY4742 (met5, met14 and met16) were purchased from EUROSCARF. Composition of SCD media: 0.17% yeast nitrogen base (BD Diagnostics; without ammonium sulfate and amino acids), 0.5% $(NH_4)_2SO_4$, 30mg/L of all amino acids (except 80mg/L histidine and 200mg/L leucine), 30mg/L adenine, and 320mg/L uracil with the indicated amounts of glucose (0.5% for DR, and 2% for standard conditions, respectively). All amino acids were purchased from Serva (research grade, ≥ 98.5%). For chronological aging experiments, cells were inoculated to an OD600 of 0.05, and grown at 28°C in SCD media. At the indicated time points, cell survival was determined by clonogenicity: Cell cultures were counted with a CASY cell counter (Schärfe System) and 500 cells were plated on YPD agar plates (at least 3 independent cultures were evaluated) and subsequently colony forming units

counted and values normalized to survival at day one. For chronological aging experiments with externally added H2S-releasing substances, GYY4137 (Sigma) dissolved in DMSO was added to BY4742 cultures at time of inoculation at a final concentration of 100μM. In addition, NaHS (Sigma) was added at time points 6, 24 and 48hrs after inoculation at concentrations of 5 μM at each time point. DMSO-treated BY4742 strain served as control.

Statistical Analyses

Microsoft Excel and GraphPad Prism were used for statistical analysis. Graphical data are displayed as means ± SEM and statistical significance assessed by GraphPad Prism using Student's t tests to compare values and one-sample t test to compare means to a hypothetical value of 1 or 100 when data was normalized to the average value of the experimental control group. Error bars present in the AL control or any of the control groups where data was normalized to represents the variation among the control individual data points relative to the average of that control group. P-values less than 0.05 were deemed statistically significant.

SUPPLEMENTAL REFERENCES

Calfee-Mason, K.G., Spear, B.T., and Glauert, H.P. (2002). Vitamin E inhibits hepatic NF-kappaB activation in rats administered the hepatic tumor promoter, phenobarbital. J. Nutr. *132*, 3178–3185.

Ergul, Y., Erkan, T., Uzun, H., Genc, H., Altug, T., and Erginoz, E. (2010). Effect of vitamin C on oxidative liver injury due to isoniazid in rats. Pediatr. Int. *52*, 69–74.

Parnell, S.E., Sulik, K.K., Dehart, D.B., and Chen, S.Y. (2010). Reduction of ethanol-induced ocular abnormalities in mice through dietary administration of N-acetylcysteine. Alcohol *44*, 699–705.

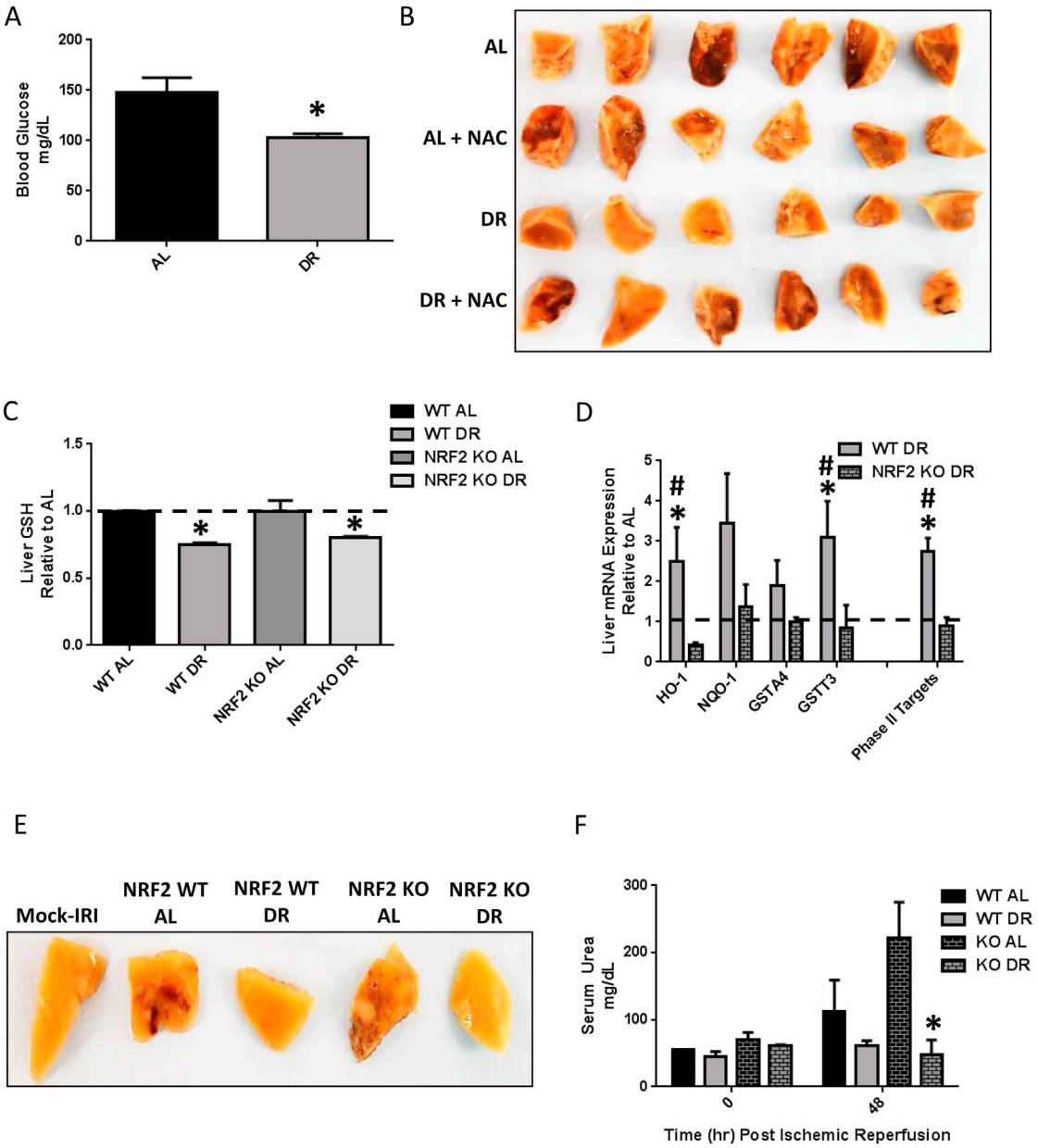

Figure S1. NAC Abrogates Benefits of DR against Acute Stress Independent of NRF2, Related to Figure 1

(A) Blood glucose following 1wk of preconditioning on the indicated diet; n = 5/group.

(B) Photographs of liver lobes (1x magnification) fixed 24hrs after reperfusion from mice fed ad libitum (AL) or 50% restricted (DR) with or without NAC supplementation as indicated.

(C) GSH levels in livers of NRF2 WT and KO mice on AL or DR regimens as indicated; n = 3-4/group.

(D) Hepatic expression of NRF2 gene targets after 1wk of DR in WT or NRF2 KO animals as indicated and expressed relative to the same genotype fed AL; n = 4/group.

(E) Photographs of liver lobes (1x magnification) fixed 24hrs after reperfusion from WT or NRF2KO mice preconditioned on AL or DR regimens as indicated; n = 7-12/group.

(F) Serum urea after renal IRI in WT or NRF2KO mice preconditioned on AL or DR regimens as indicated; n = 3-4/group. Asterisk indicates the significance of the difference compared to WT AL, and pound sign compared to NRF2KO AL; */#$p < 0.05$.

All error bars SEM.

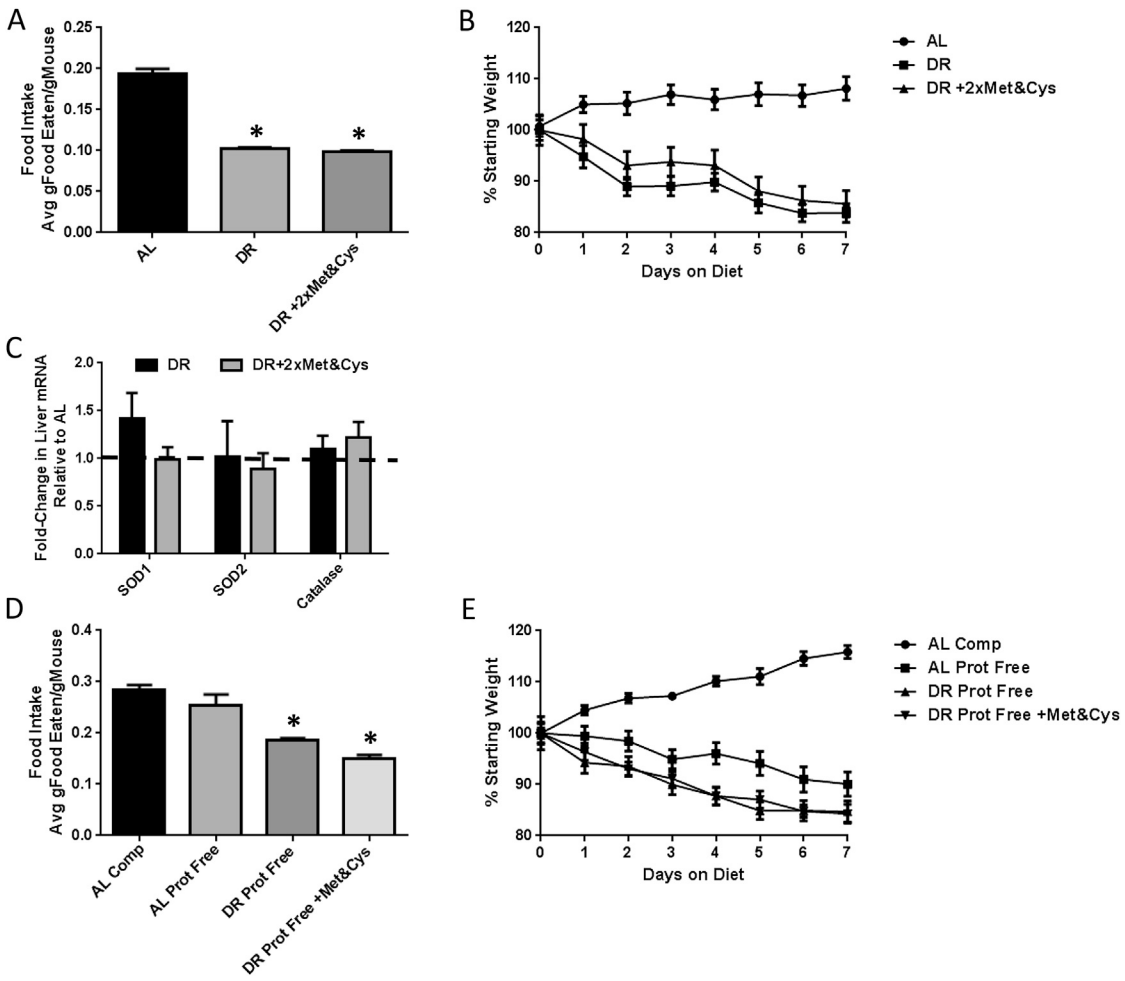

Figure S2. Sulfur Amino Acids Control the Benefits of DR and PR, Related to Figure 2

(A) Food intake during the 7d preconditioning period on the indicated complete diet fed ad libitum (AL) or 50% restricted (DR) with or without supplementation of 2xMet&Cys as indicated and expressed as grams food eaten per gram of mouse body weight; n = 5/group. Asterisk indicates the significance of the difference versus the AL group; *$p < 0.05$.

(B) Average daily weight of mice on the indicated diet during the 7d preconditioning period; n = 5/group.

(C) Changes in FOXO target gene expression in DR and DR +2xMet&Cys diet groups expressed relative to the AL group; n = 3-4/group.

(D) Food intake during the 7d preconditioning period on the indicated complete or protein free diets fed AL or restricted 35% (DR) with or without supplementation of Met&Cys as indicated and expressed as grams eaten per gram of mouse; n = 5/group. Asterisk indicates the significance of the difference versus the AL group on a complete diet; *$p < 0.05$.

(E) Average daily weight of mice on the indicated diet during the 7d preconditioning period; n = 5/group.

All error bars SEM.

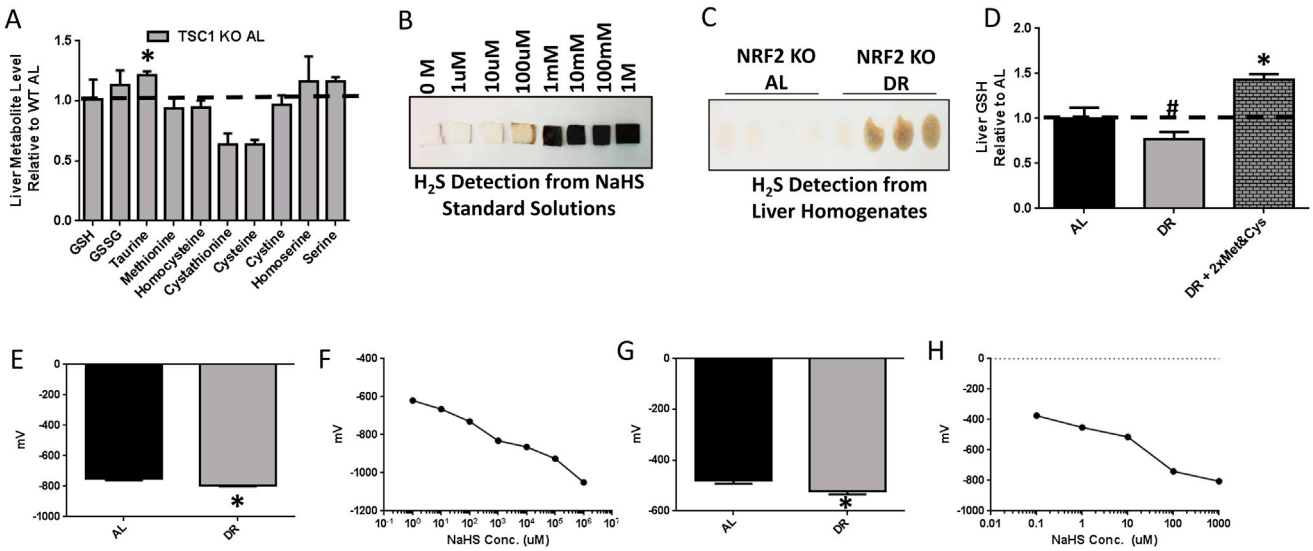

Figure S3. DR Stimulates Endogenous H_2S Production via the TSP, Related to Figure 3

(A) Liver metabolite levels in LTsc1KO mice on AL complete diet expressed relative to the average value of that metabolite in the WT AL group; n = 5/group.

(B) Lead sulfide standard curve generated with NaHS dissolved in water at the indicated concentration for detection of H_2S using lead acetate paper.

(C) H_2S production from NRF2KO mice fed AL or restricted 50% (DR) for 1wk as indicated using the lead sulfide method. Each sample represents an individual mouse; n = 4/group.

(D) Hepatic GSH levels of mice on the indicated diet for 1wk relative to the AL group; n = 3-5/group. Asterisk indicates the significance of the difference relative to the AL group, and the pound sign relative to DR +2xMet&Cys; */#$p < 0.05$.

(E and F) Microsulfide probe-based mV reading of H_2S production from extracts of livers from mice on the indicated diet for 1wk (E) and the corresponding standard curve using NaHS dissolved in water at the indicated concentration (F).

(G and H) Microsulfide probe-based mV reading of endogenous H_2S present in liver lobes of mice on the indicated diet (n = 3 mice/group and 2 lobes/animal, (G) and the corresponding standard curve using NaHS dissolved in water at the indicated concentration (H). Asterisk indicates the significance of the difference relative to the AL group; *$p < 0.05$.

All error bars SEM.

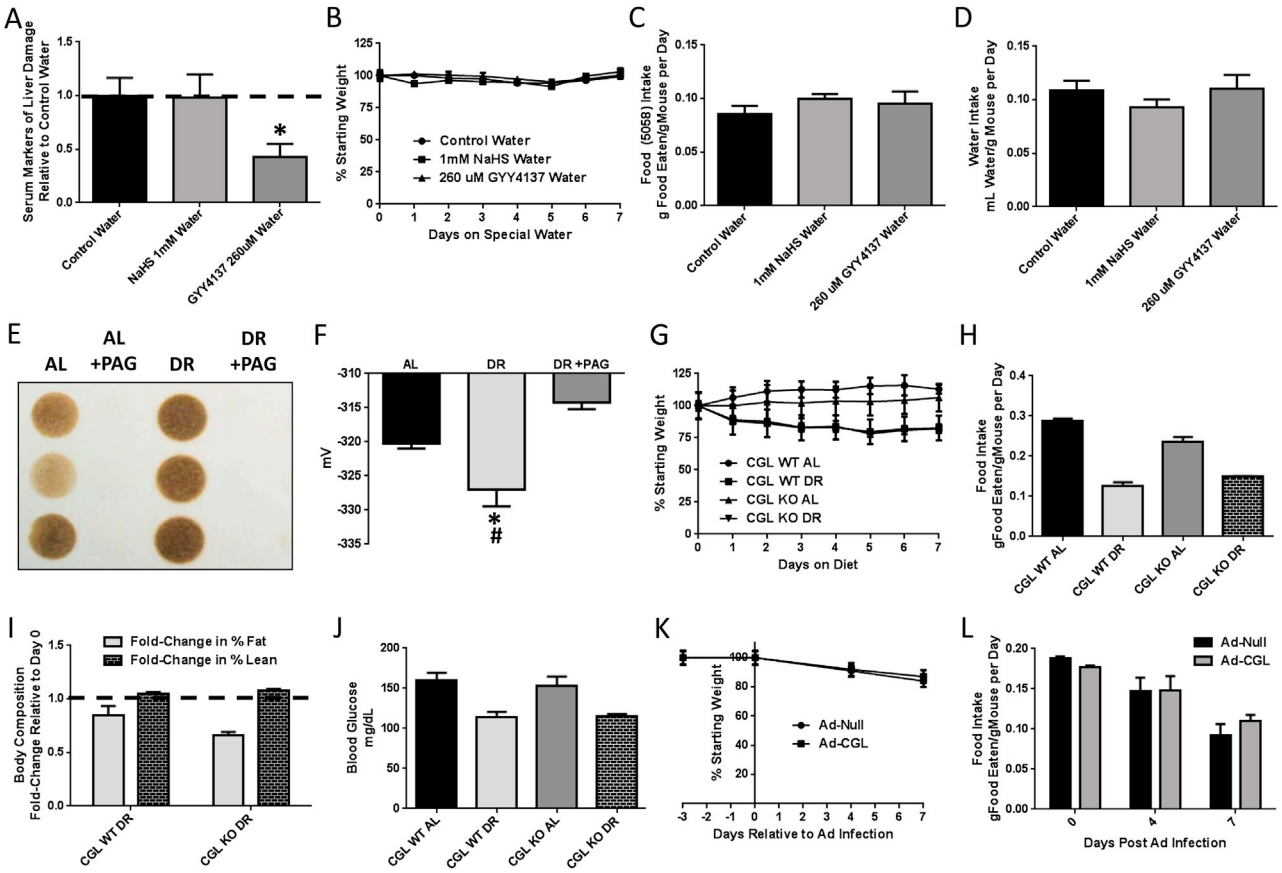

Figure S4. H_2S Is Necessary and Sufficient to Confer DR Benefits against Hepatic IRI, Related to Figure 4

(A–D) Combined serum markers of liver damage 3 and 24hrs after reperfusion (A), animal weight (B), food intake (C) and water intake (D) of mice (n = 4/group) treated with extended slow-release H_2S donor GYY4137 or short-lived NaHS in the drinking water as indicated for 1wk prior to hepatic IRI. Asterisk indicates the significance of the difference versus the Control water group; *p < 0.05.

(E) H_2S production using the lead sulfide method in extracts of livers prepared 24hrs after hepatic IRI from animals preconditioned on AL or DR regimens with or without PAG as indicated for 1wk. Each circle represents H_2S production from an individual animal.

(F) Microsulfide probe-based mV readings of endogenous H_2S in livers of animals preconditioned on AL or DR regimens with PAG as indicated for 1wk; n = 4/group. Asterisk indicates the significance of the difference versus the AL group, and pound sign relative to DR +PAG; */#p < 0.05.

(G–J) Body mass (G), food intake (H), changes in body composition (I) and blood glucose (J) in in WT or CGLKO mice preconditioned on the indicated diet for 1wk; n = 5-8/group. (K and L) Body mass (K) and food intake (L) of AL fed animals infected with the indicted virus prior to and up to 7d post infection; n = 6/group.

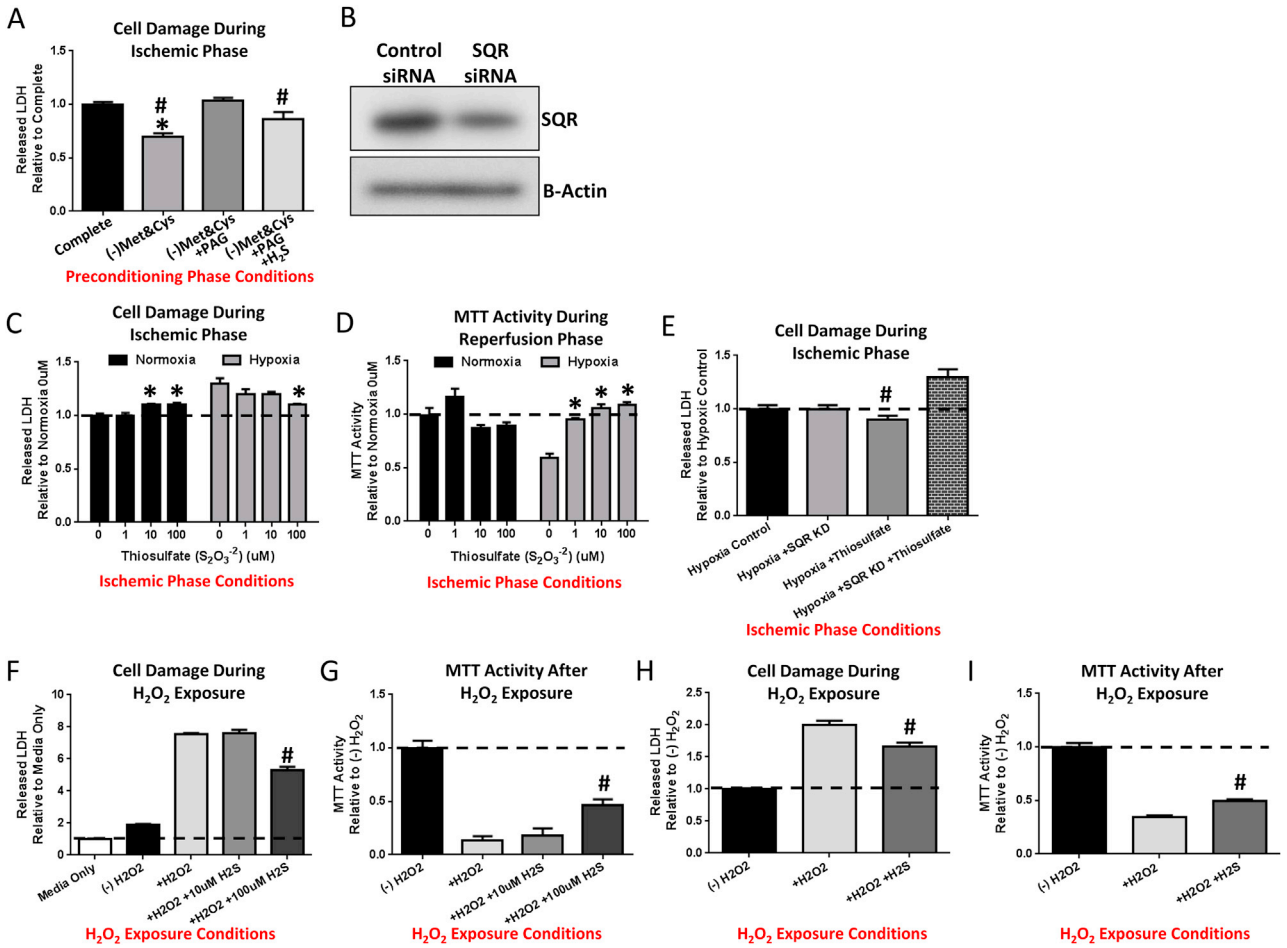

Figure S5. Mitochondrial SQR Is Required for Cytoprotective Effects of H_2S during Ischemia, Related to Figure 5

(A) LDH release during the ischemic phase in Hepa1-6 cells preconditioned overnight in complete media or media lacking Met, Cys and serum (-Met&Cys) with or without PAG as indicated; H_2S was added during the ischemic phase where indicated. Asterisk indicates the significance of the difference relative to the Complete group, and the pound symbol indicates the significance of the difference relative to the –Met&Cys +PAG group; */# $p < 0.05$.

(B) Immunoblot of SQR in Hepa1-6 cells 48hr after siRNA targeting mouse SQR or scrambled control.

(C and D) Cell autonomous effects of exogenous thiosulfate ($S_2O_3^{-2}$) on simulated IRI in Hepa1-6 cells. Thiosulfate was added during the ischemic phase and removed during the reperfusion phase. LDH release (C) during 3hr incubation in saline (simulated nutrient/energy deprivation) under normoxic or hypoxic (simulated ischemia) conditions in the presence of the indicated concentration of thiosulfate; MTT activity (D) upon readdition of complete media without thiosulfate under normoxic conditions (simulated reperfusion). Asterisk indicates the significance of the difference between the indicated thiosulfate dose and no thiosulfate addition within normoxic or hypoxic treatment groups; *$p < 0.05$.

(E) LDH release from Hepa1-6 cells with or without SQR KD during simulated ischemia ± exogenous thiosulfate ($S_2O_3^{-2}$). Pound sign indicates the significance of the difference between control and SQR KD within a given treatment group; #$p < 0.05$.

(F and G) Effects of the indicated H_2S concentration on LDH release (F) and MTT activity (G) following 5mM H_2O_2 treatment of Hepa1-6 cells.

(H and I) Effects of 100uM H_2S addition on LDH release (H) and MTT activity (I) following 1mM H_2O_2 treatment of primary mouse vascular smooth muscle cells. Pound sign indicates the significance of the difference between H_2O_2 alone versus H_2O_2 plus H_2S; #$p < 0.05$.

All error bars SEM.

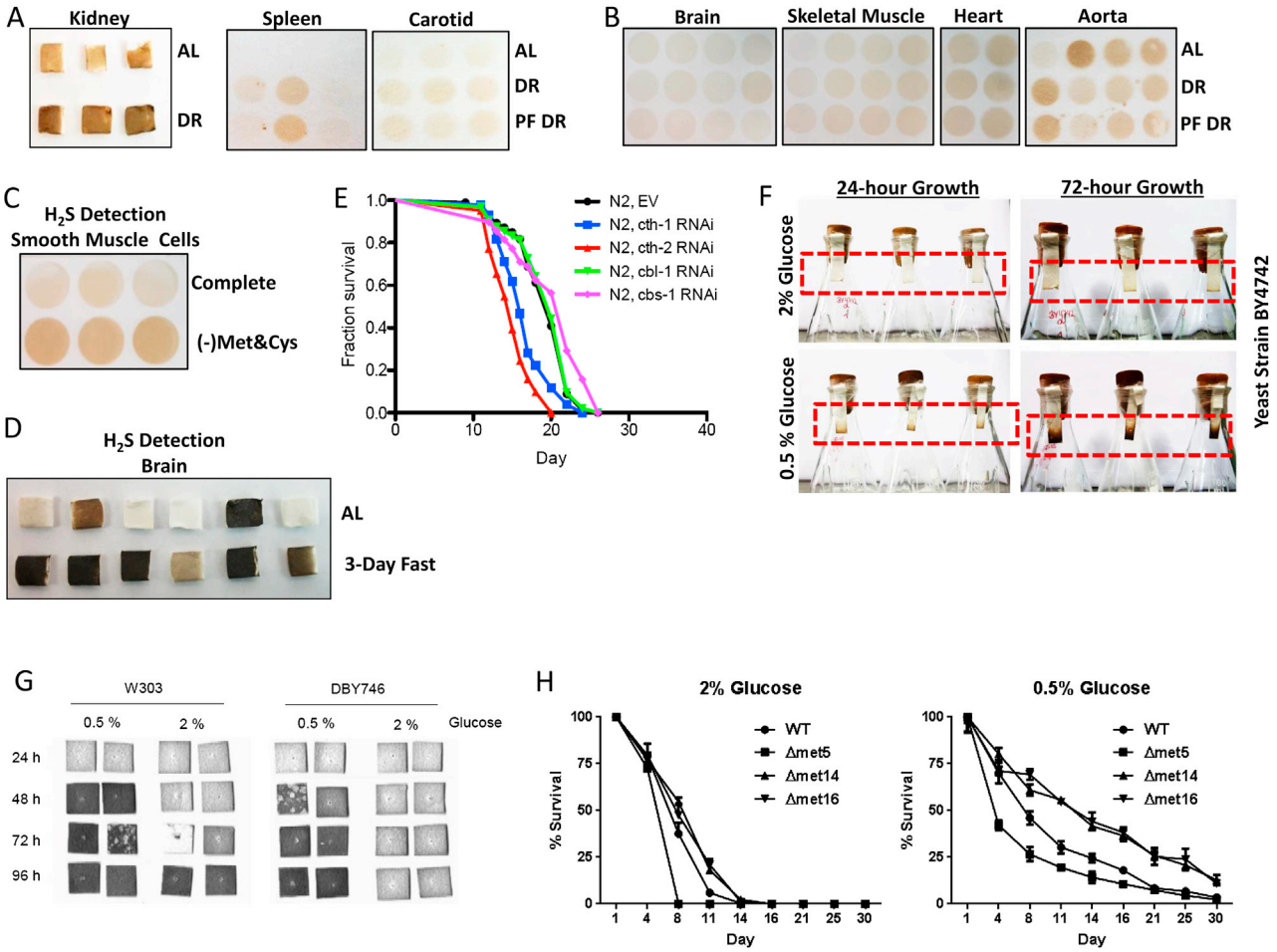

Figure S6. Increased Endogenous H_2S Production in Diet-Induced Longevity Extension Models Crosses Evolutionary Boundaries, Related to Figure 6

(A and B) H_2S production capacity in extracts of kidney, spleen, carotid artery, brain, skeletal muscle, heart, and aorta from mice with AL or restricted access (DR) to complete or protein free (PF) diets as indicated. Extracts were normalized for protein content or organ weight; each circle represents H_2S production from an individual animal as measured by the lead sulfide method.

(C) H_2S production from primary aorta smooth muscle cells after overnight preconditioning in complete or media lacking Met&Cys.

(D) H_2S production from brains after AL feeding or 3d water-only fasting.

(E) Effects of RNAi-mediated knockdown of individual TSP components on longevity of wild-type N2 worms compared to empty vector (EV).

(F and G) H_2S production from three different wild-type yeast strains as a function of glucose concentration and time in culture as detected by black lead sulfide accumulation on lead acetate strips placed in the growth flasks (F) or square lead acetate papers inserted into the caps of the growth flasks for the indicated time (G).

(H) Chronological lifespans of the indicated WT or sulfur assimilatory pathway mutants grown in 2.0% (left) or 0.5% (right) glucose.

All error bars SEM.